Impact of PDFs on precision DY measurements

Aaron Armbruster, Maarten Boonekamp,
Stefano Camarda, Daniel Froidevaux

CERN

March 28, 2018

Motivation

- PDFs have been, or are becoming, a limiting systematic in many precision DY measurements, such as m_W and $\sin^2\theta_W$
- These slides present studies on the impacts of PDFs on these measurements
- $\sin^2\theta_W$
  - Typically inferred from forward-backward asymmetry A_{FB}, or related angular coefficient A_4, in Z-boson events
    - Studies here focus on A_4, will refer to this from now on, though studies with A_{FB} should yield comparable results
  - PDF uncertainties on A_4 are small, however PDF uncertainties on predictions for A_4 may mimic variations of $\sin^2\theta_W$ near the Z-mass pole where we're most sensitive to $\sin^2\theta_W$
  - Profiling PDF uncertainties in-situ can significantly reduce the systematic component on the extracted $\sin^2\theta_W$
    - Sensitivity to $\sin^2\theta_W$ increases with Z-boson rapidity, since dilution effects decrease at high y^Z
    - Above and below the Z-mass pole A_4 becomes less sensitive to $\sin^2\theta_W$ and more sensitive to PDFs
    - Profiling A_4 simultaneously vs m^Z and y^Z can significantly reduce underlying PDF uncertainties while increasing $\sin^2\theta_W$ sensitivity, as previous measurements have shown
  - Here we show closure tests between different PDF sets with and without PDF profiling, both on the observable A_4 and on $\sin^2\theta_W$

$$\frac{d\sigma}{dp_T^Z\, dy^Z\, dm^Z\, d\cos\theta\, d\phi} = \frac{3}{16\pi}\frac{d\sigma^{U+L}}{dp_T^Z\, dy^Z\, dm^Z}$$
$$\Big\{(1+\cos^2\theta) + \frac{1}{2}A_0(1-3\cos^2\theta) + A_1 \sin 2\theta \cos\phi$$
$$+\frac{1}{2}A_2 \sin^2\theta \cos 2\phi + A_3 \sin\theta \cos\phi + \boxed{A_4}\cos\theta$$
$$+A_5 \sin^2\theta \sin 2\phi + A_6 \sin 2\theta \sin\phi + A_7 \sin\theta \sin\phi\Big\}$$

$$\sigma^{U+L,L,T,I} \propto (v_\ell^2 + a_\ell^2)(v_\ell^2 + a_q^2)$$
$$\sigma^{P,A} \propto v_\ell a_\ell v_q a_q$$
$$\sigma^{7,8} \propto (v_\ell^2 + a_\ell^2)(v_q a_q)$$
$$\sigma^{9} \propto v_\ell a_\ell (v_q^2 + a_q^2),$$

$$A_4 = \sigma^P / \sigma^{U+L}$$

$$v_{l,f} \sim 2*T_3^{l,f} - 4*q_{l,f}*\boxed{\sin^2\theta_W}$$

Motivation

- PDFs have been, or are becoming, a limiting systematic in many precision DY measurements, such as m_W and $\sin^2\theta_W$
- These slides present studies on the impacts of PDFs on these measurements
- mW
  - Fixed order predictions, such as those used in PDF fits, have unphysical divergent description of boson transverse momentum in the low pT region
  - Fiducial selections on leptons increase sensitivity to this unphysical boson pT
  - Parton shower MCs used to perform unfolded fiducial differential measurements restore a proper physical behaviour of the boson pT distribution, similarly to state-of-the-art resummed predictions which will be discussed in this talk
  - Profiling PDF uncertainties using measurements to these fiducial predictions can introduce non-closures when porting results back into data/MC comparisons
- References to relevant measurements in ATLAS:
  - ATLAS W-mass: https://arxiv.org/abs/1701.07240
  - ATLAS angular coefficients: https://arxiv.org/abs/1606.00689
  - ATLAS Z3D: https://arxiv.org/abs/1710.05167
  - Results here will be available in a pub note to be made public soon

Predictions of A_4 vs m^Z and y^Z

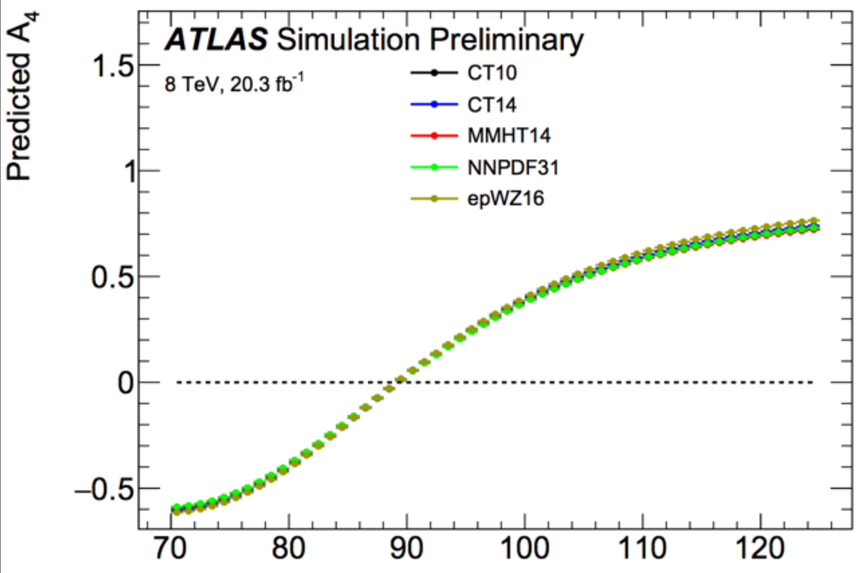

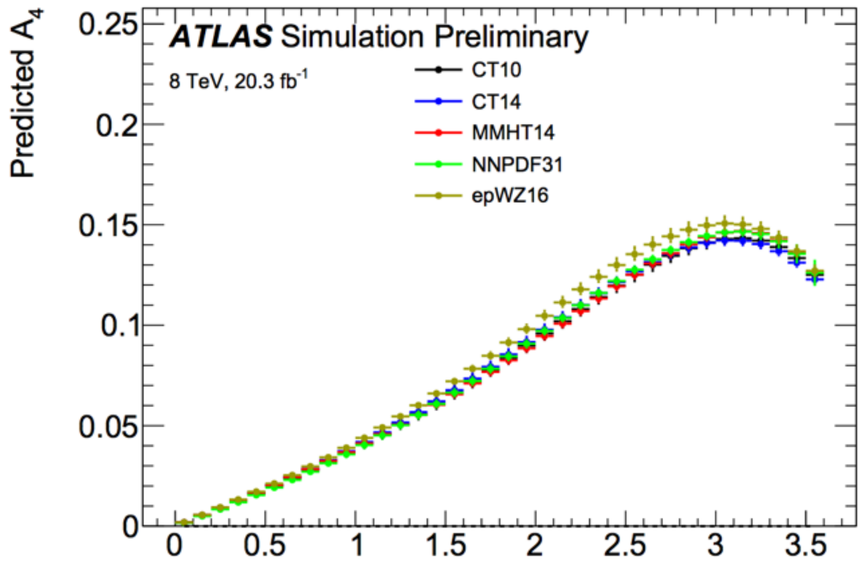

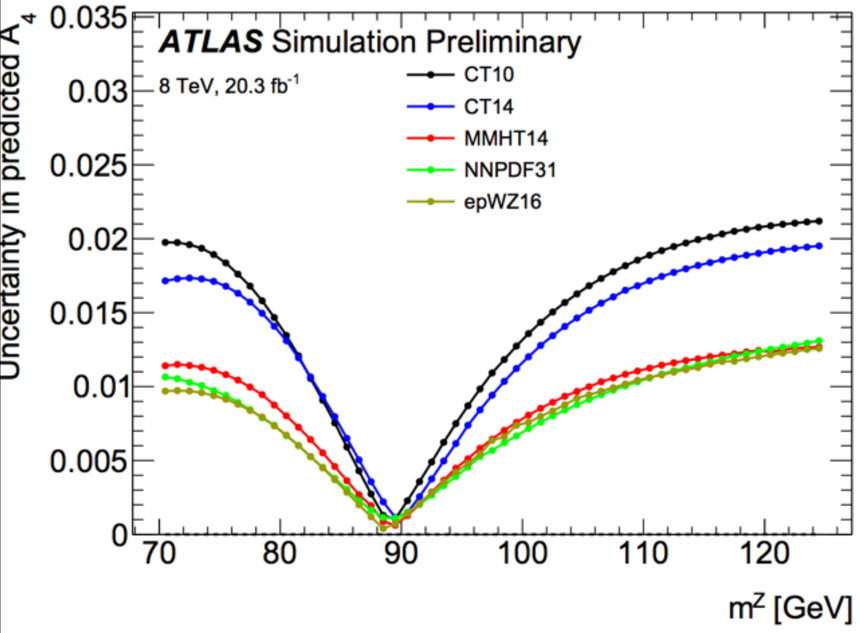

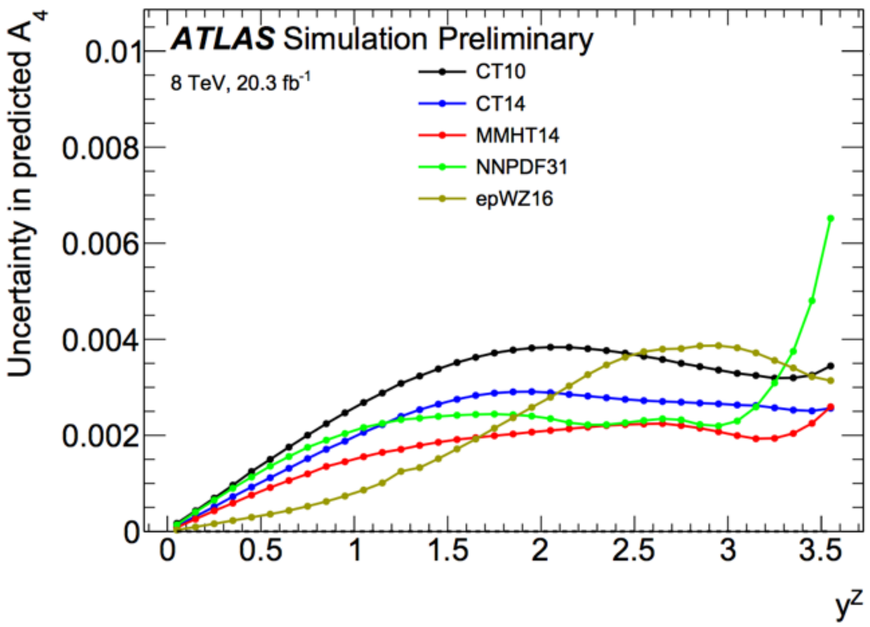

- Fixed-order predictions of A_4 using optimized version of DYRES
  - NLO QCD
  - LO EW
  - pdg $\sin^2\theta_W$ for central value
- A_4 largest at $y^Z \sim 3$, shape vs y^Z driven by dilution effects
- Uncertainty on A_4 largest above and below the mass pole

Predictions of A_4 vs m^Z and y^Z

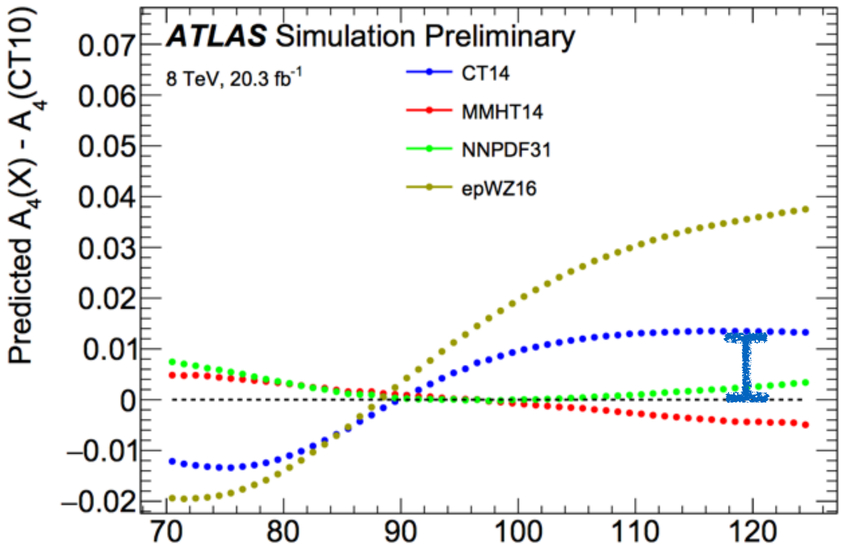

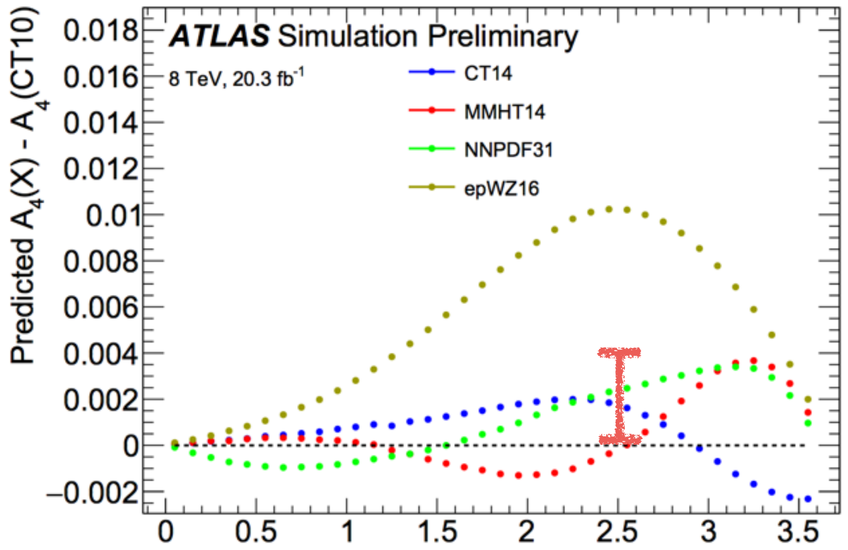

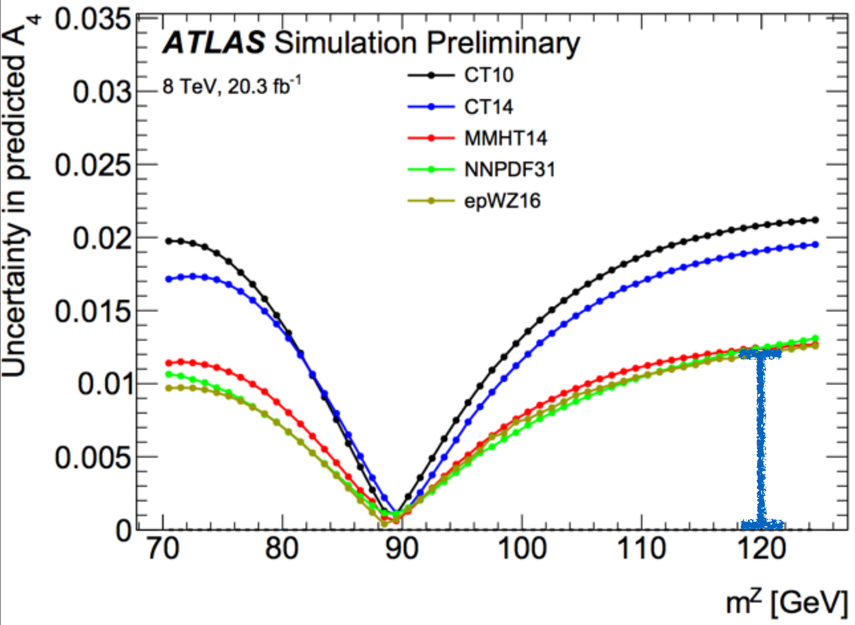

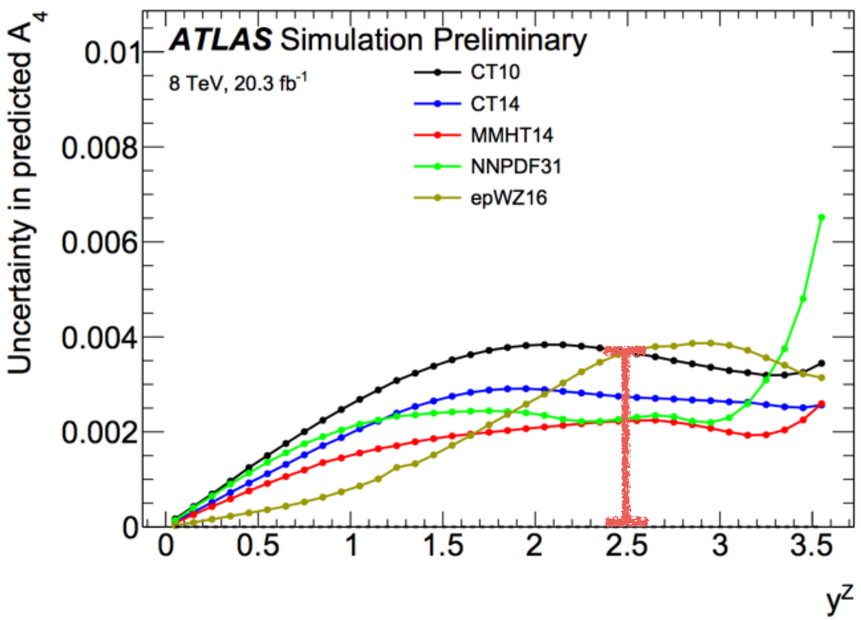

- Most predictions within 1σ of each other
- ATLAS-epWZ16 is 2-3σ from others at high y^Z where we have highest sensitivity to $\sin^2\theta_W$
- Differences between PDF sets in m^Z are generally different in sign below and above the pole, while changes in A_4 from $\sin^2\theta_W$ variations peak at the pole and are the same sign above and below the pole
- Differences in y^Z can sometimes have a different sign above and below 2.5 or so

Comparing raw PDFs between sets

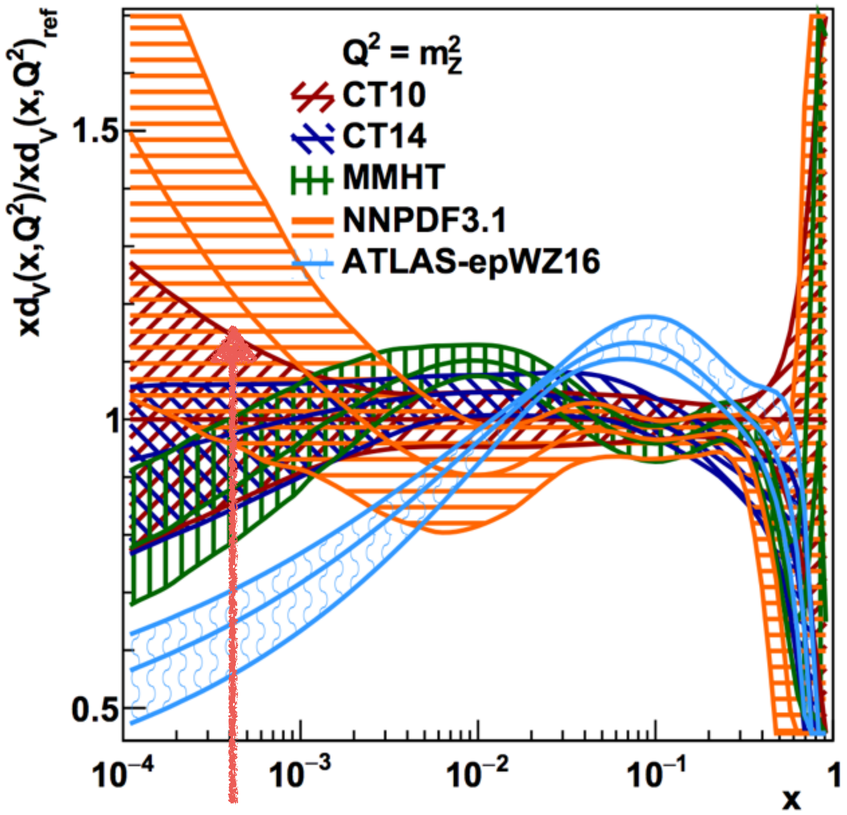

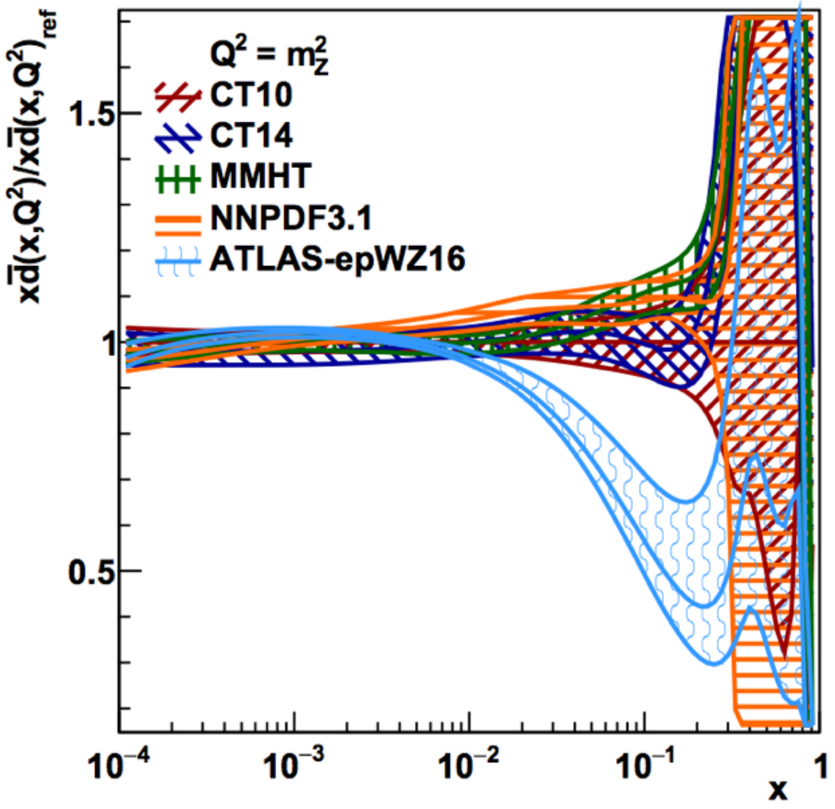

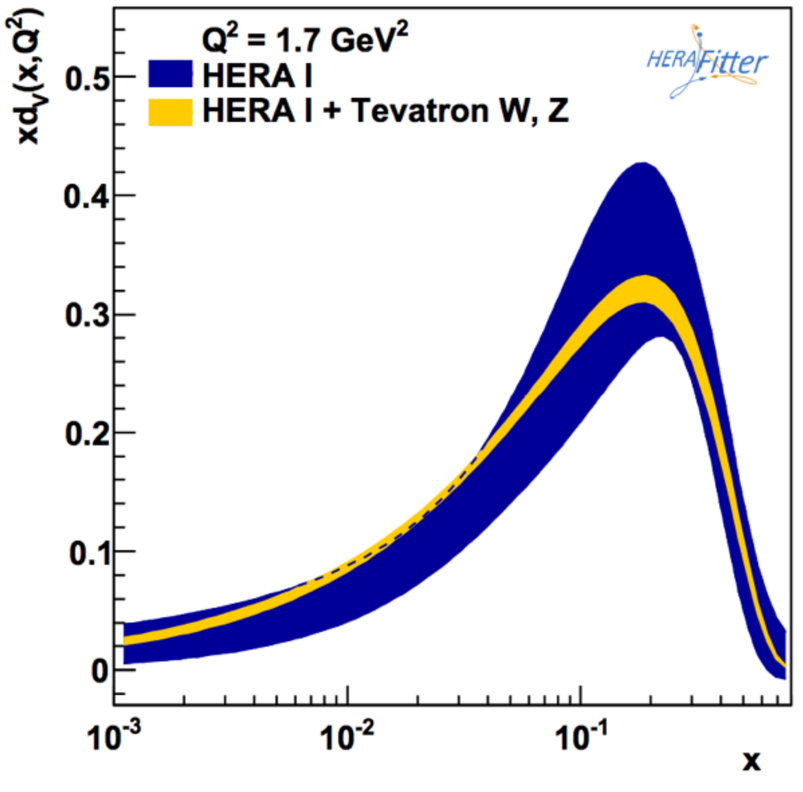

https://arxiv.org/abs/1503.05221

- Difference in A_4 between epWZ16 and others driven by difference in d-valence distribution
- This is largely constrained by Tevatron W-asymmetry measurements in “global” PDF sets
- Possibly due to not-flexible-enough parametrization used within the set

Correlation between predicted A_4 in different y^Z bins

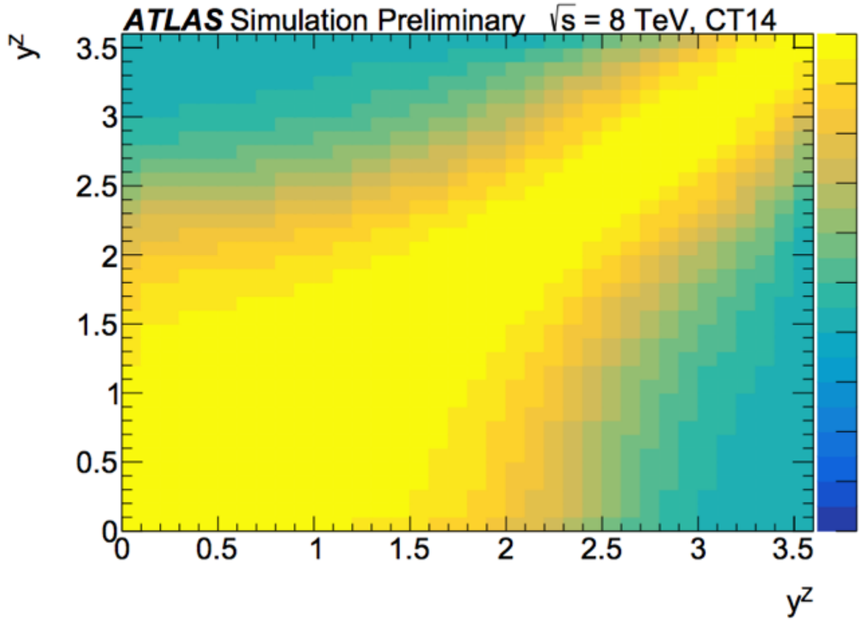

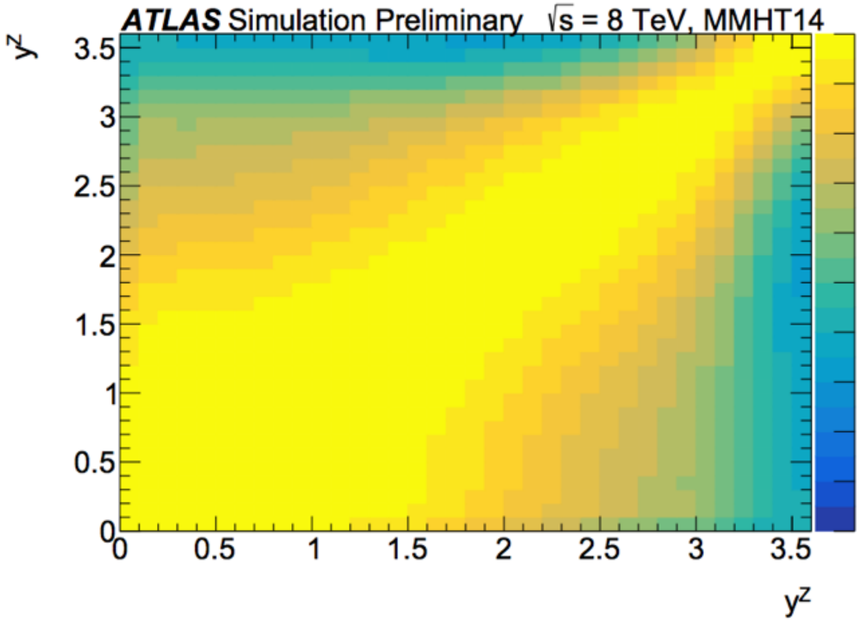

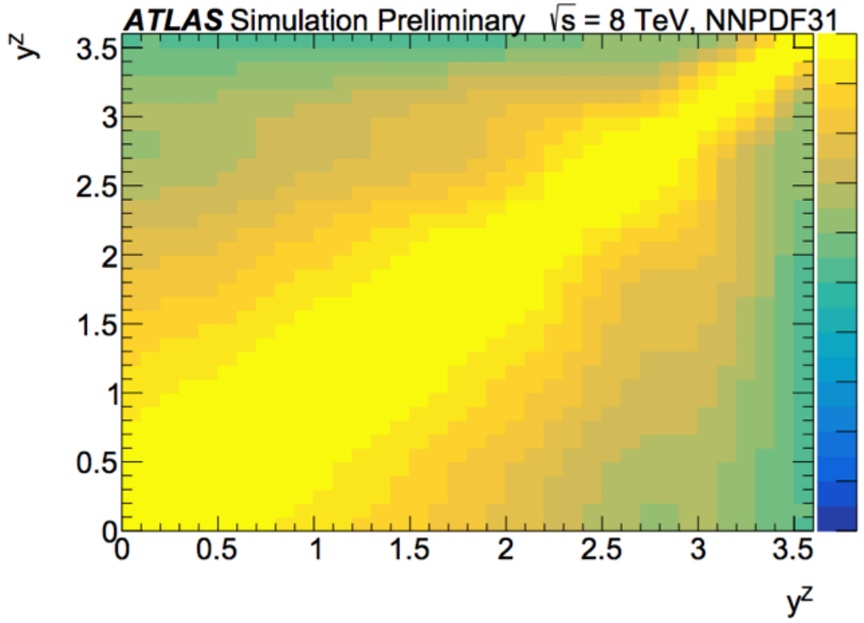

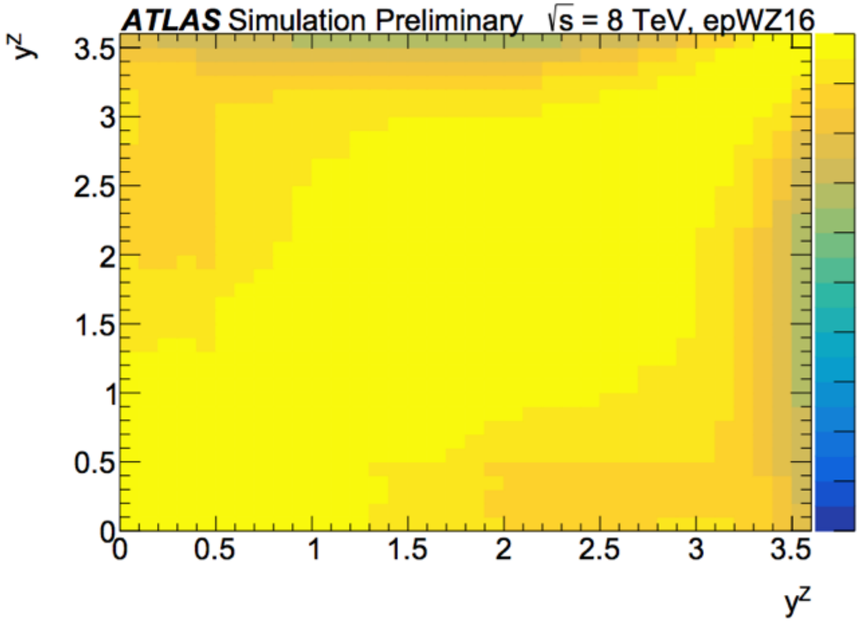

- Correlation of PDF uncertainty on predicted A_4 in bins of y^Z
- Helps to understand a bit the effects of PDF profiling on the shape of the predictions in y^Z, and the limitations of the profiling to provide post-fit closure between PDF sets
- Also illustrates (sometimes largely) different correlation structure between PDF sets
- Correlations in m^Z (not shown) are much simpler, nearly 100% anti-correlated between regions above and below the pole

A_4 to $\sin^2\theta_W$

- Performing fits to pseudo-data based on different PDF sets using A_4-style measurement, in 12 analysis-level bins
  - m^Z: [70, 80, 100, 125] GeV
  - $|y^Z|$: [0, 0.8, 1.6, 2.5, 3.6]
  - $ee_{CC}+\mu\mu_{CC}$ channels cover $|y^Z| < 2.5$: Two electrons with $|\eta| < 2.5$
  - ee_{CF} channel covers $1.6 < |y^Z| < 3.6$: One electron with $|\eta| < 2.5$, one with $2.5 < |\eta| < 4.9$
- Fits performed as follows:
  - Measure A_4 in pseudo-data (verified that this recovers input A_4), based on expected stats at 8 TeV, along with stat correlation
  - Use predictions to compute linear dependence of A_4 vs $\sin^2\theta_W$, and all PDF variations of this, in each bin "n"
    - $A_4^n(\sin^2\theta_W, \theta) = a_n(\theta)*\sin2\theta W + b_n(\theta)$: **"Interpretation model"**
    - θ are nuisance parameters encapsulating PDF eigenvector variations, and in the case of epWZ16 other param. and theo. sys
  - Fit A_4^n spectrum to extract $\sin^2\theta_W$, θ
  - **Can use different PDF set for pseudo-data and interpretation model to test closure between PDF sets**

- Only **statistical** uncertainties are considered at the level of A4 extraction, and **PDF uncertainties** at the level of the sin2θW extractions, to isolate the impact of the differences between PDF sets on 8 TeV-like conditions

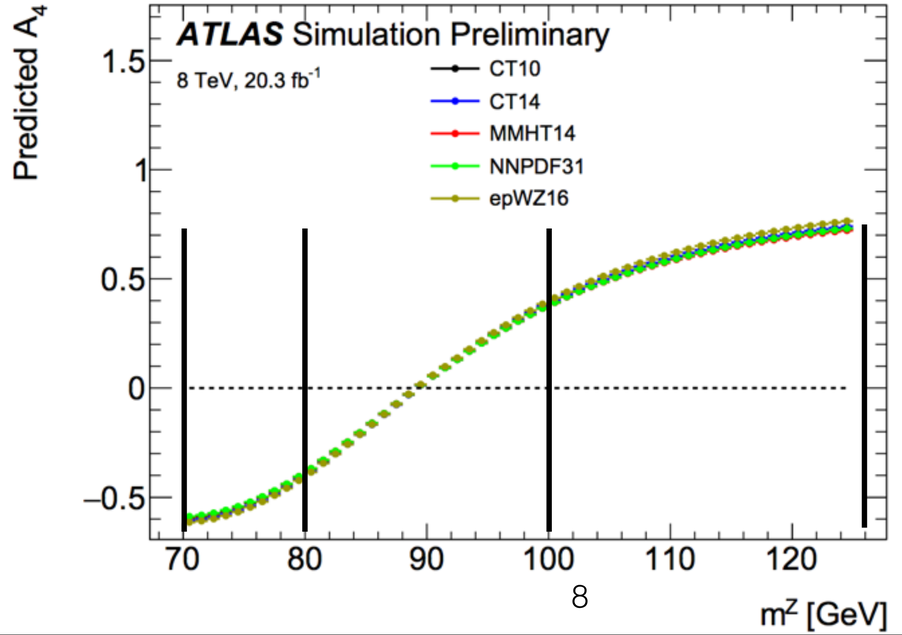

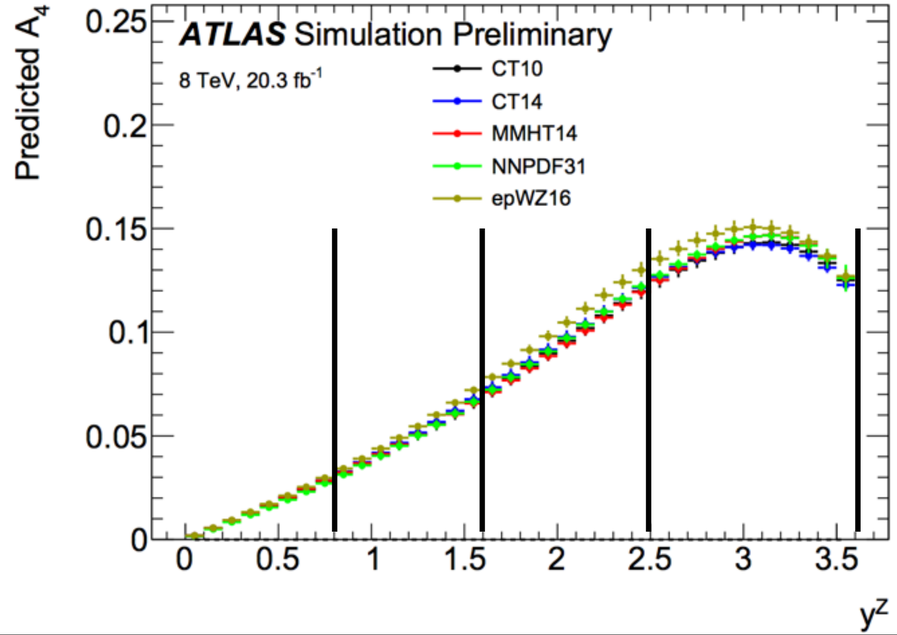

A4-level closure

- $A_4^n(\sin^2\theta_W, \theta) = a_n(\theta)*\sin^2\theta_W + b_n(\theta)$ can be computed for any m^Z, y^Z bin
- Best fit values of $\sin^2\theta_W$ and θ can be re-injected back into A_4 predictions in any binning
- Fit can be performed under three different conditions
  - $\sin^2\theta_W$ free: Test ability of sin2θW alone to cover differences between sets
  - PDF NPs free: Test ability of PDF NPs alone to cover differences
  - $\sin^2\theta_W$+PDF NPs free: Test ability of PDFs + $\sin^2\theta_W$ to cover differences
- Plots show pre- and post-fit differences between predictions
  - Prediction 1 (interp. model) + PDF unc.
  - Prediction 2 (pseudo-data) + PDF unc.
- Ideal case: PDF NPs can cover differences between PDF sets (brown matches blue)
  - Limited data statistics and DoFs in PDF EVs cause A_4-level non-closure
  - Shape vs m^Z tends to drive fit, and matches much better than shape vs y^Z
- Post-fit value of $\sin^2\theta_W$ will in general be different than injected value
  - Difference between **red** and **black** shows how much $\sin^2\theta_W$ alone will absorb differences between PDF sets
  - Difference between **green** and **brown** shows how much $\sin^2\theta_W$ will absorb these differences after PDFs are allowed to be profiled

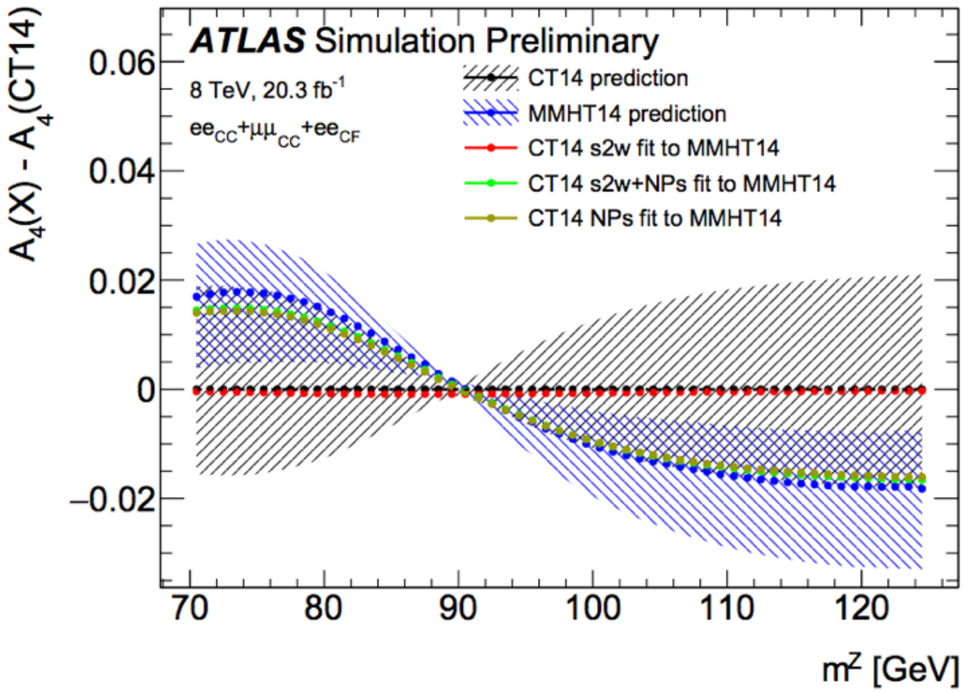

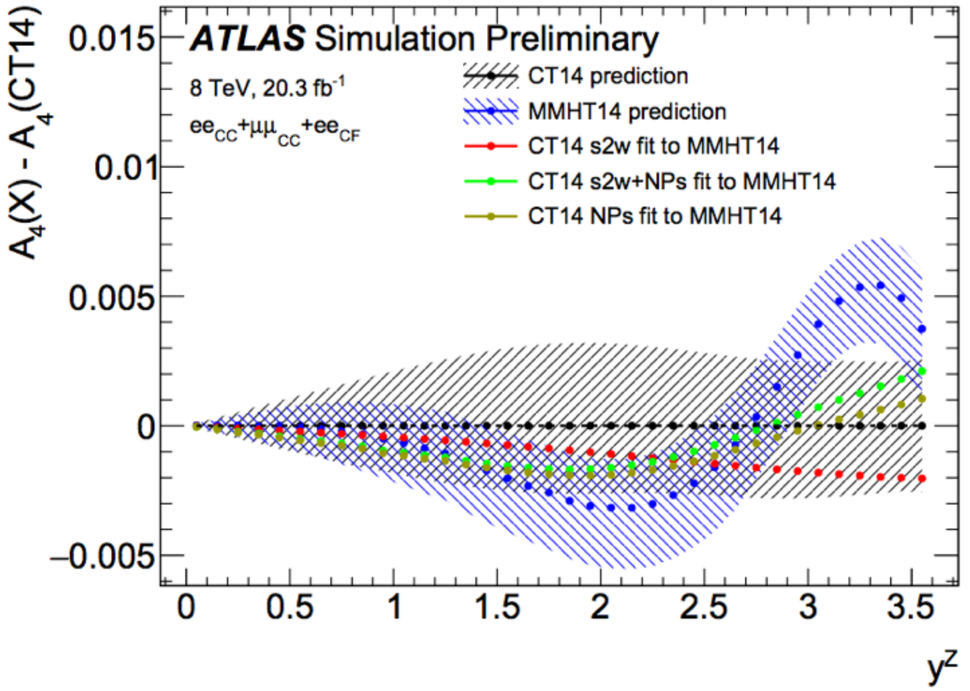

A_4-level closure

- Fits can be done also with CC channels alone, which covers only $|y^Z| < 2.5$
- Non-closure in $\sin^2\theta_W$ tends to be larger without ee_{CF}, since difference between sets are roughly monotonic at low y^Z alone
- Including high y^Z in the fit tends to stabilize non-closure, though the main motivation for including events with $|y^Z| > 2.5$ is their far greater sensitivity to $\sin^2\theta_W$

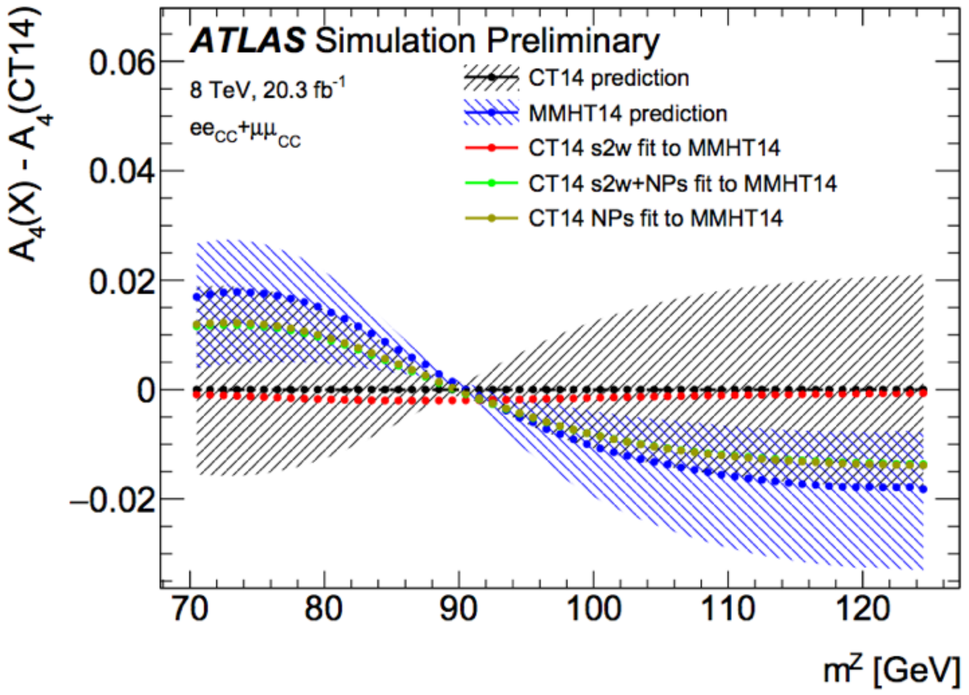

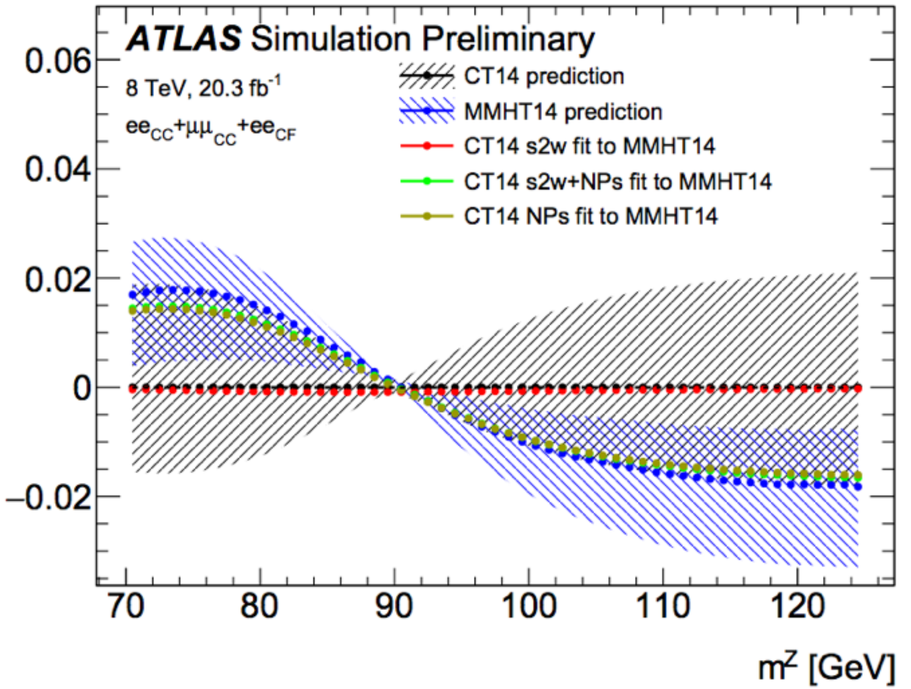

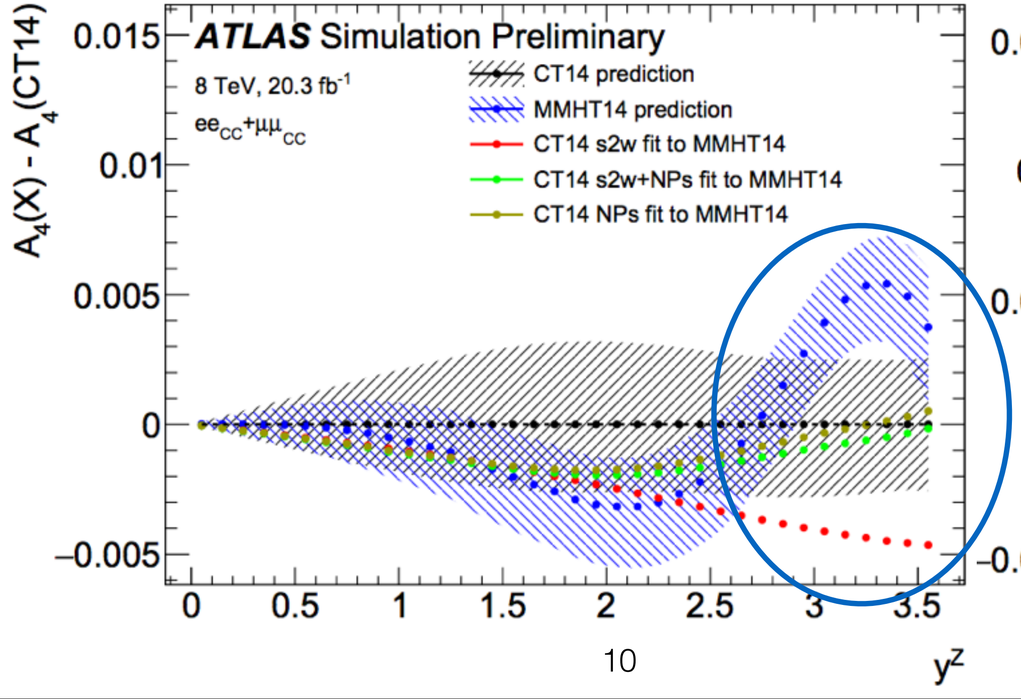

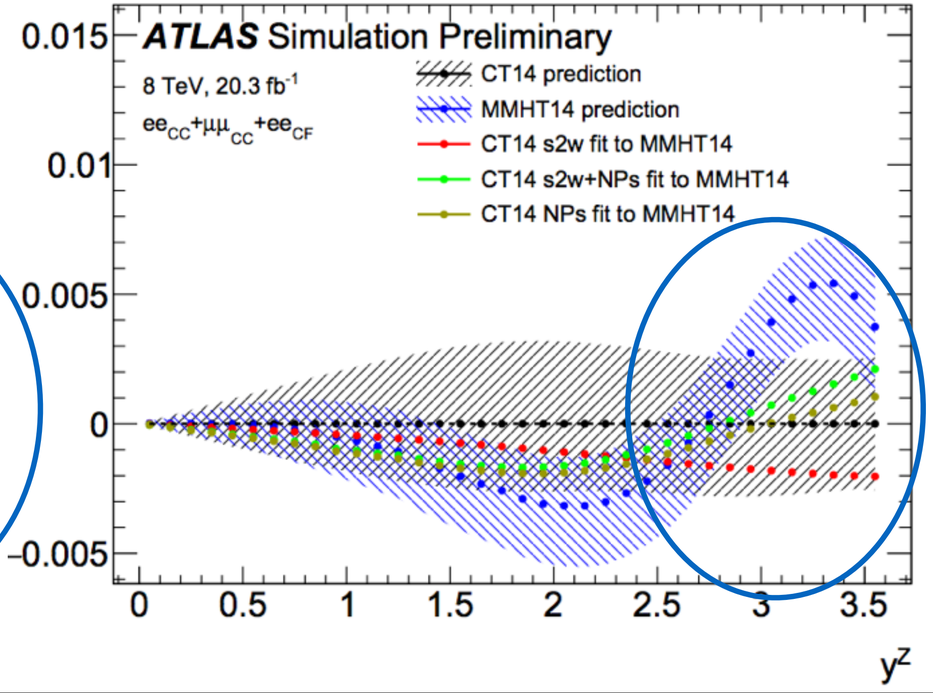

A_4-level closure

- Mirror of this can be done: swap PDF sets used for interp. and pseudo-data
- Red curve is usually quite symmetric, but differences in PDF uncertainties cause some asymmetries in post-fit closure

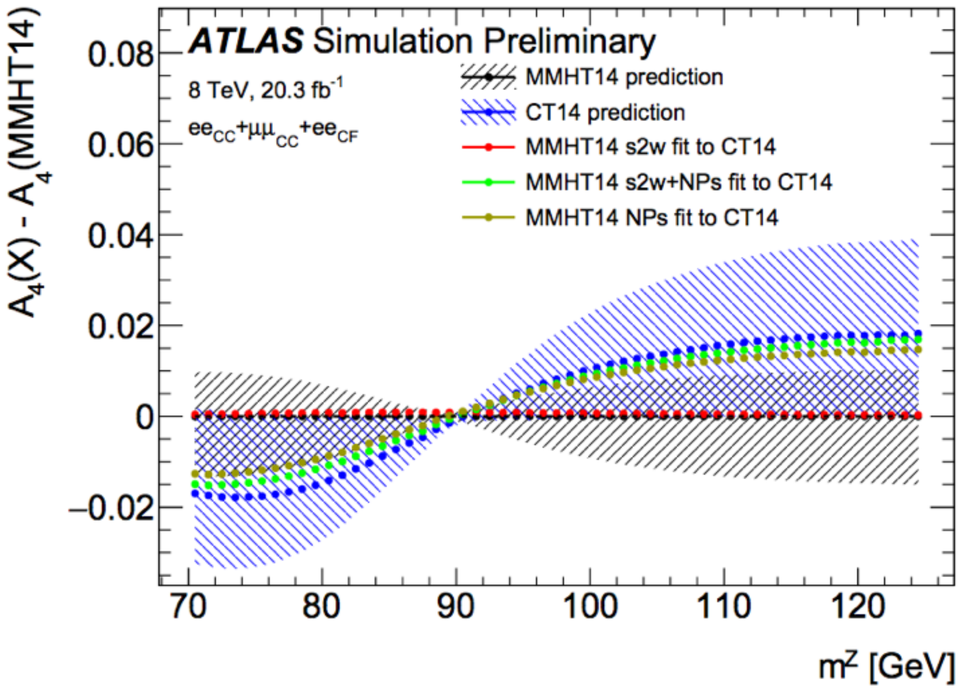

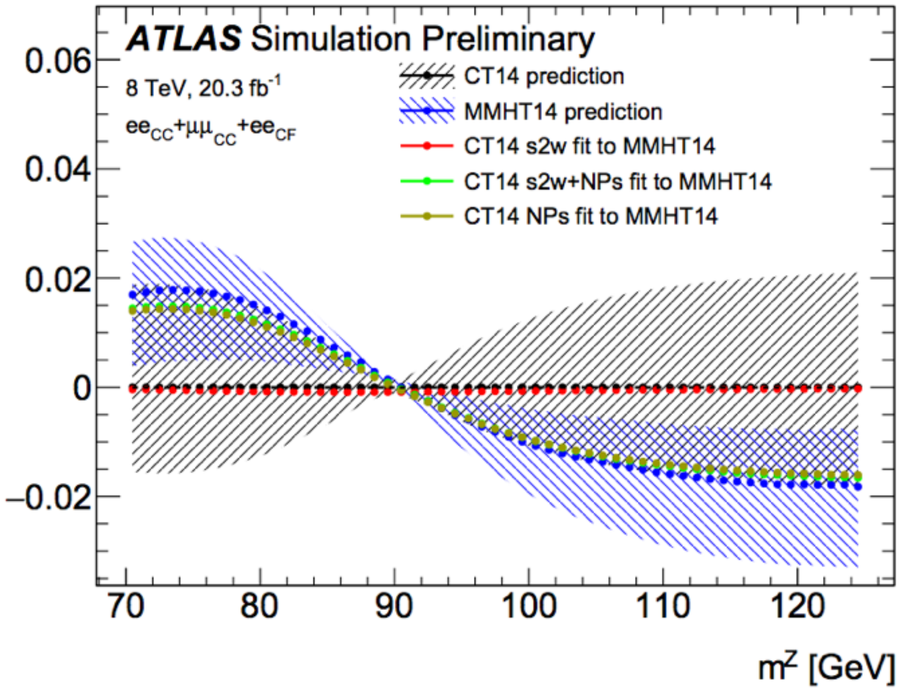

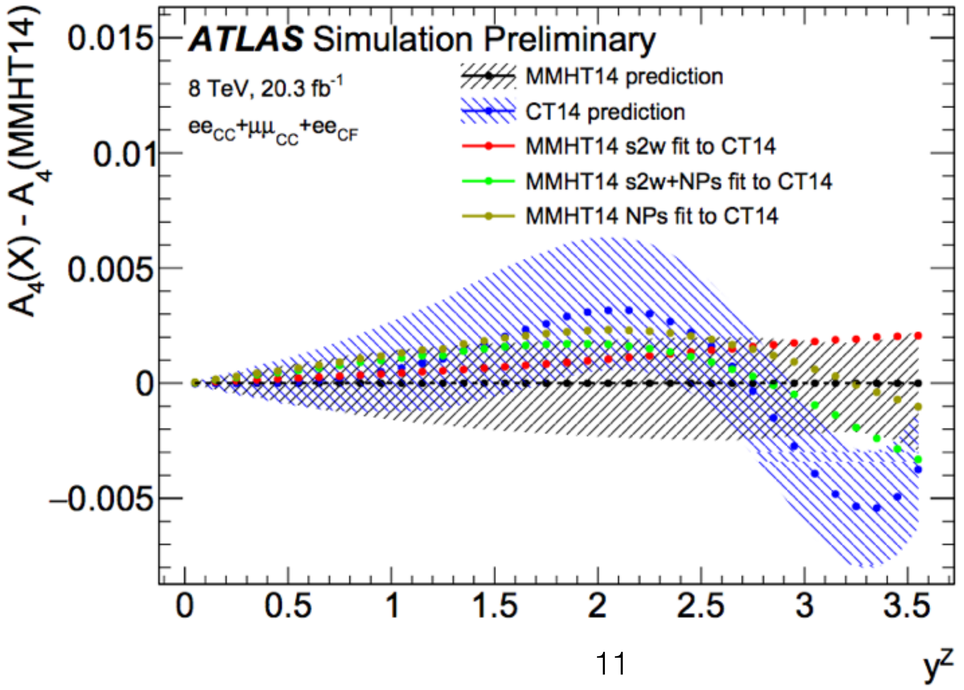

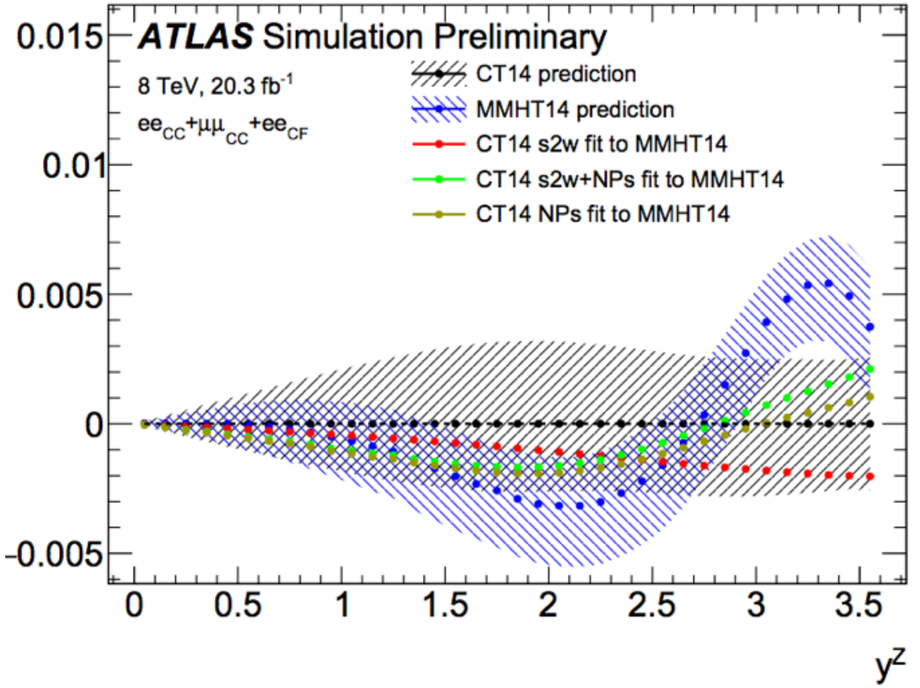

epWZ16 set

- As expected from differences in predictions, epWZ16 does not close well with other sets
- Very large differences between both red and black, and green and brown:
  - PDF NPs not able to absorb differences between sets
  - $\sin^2\theta_W$ tries to cover too much of the difference

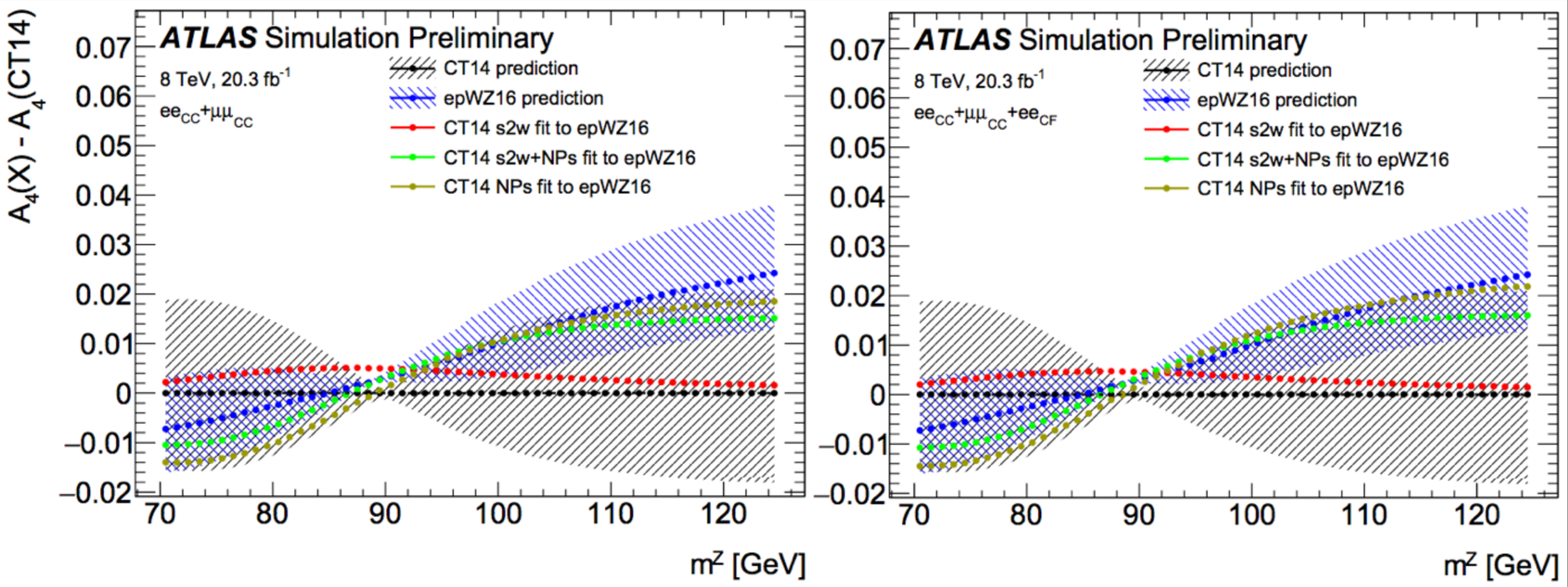

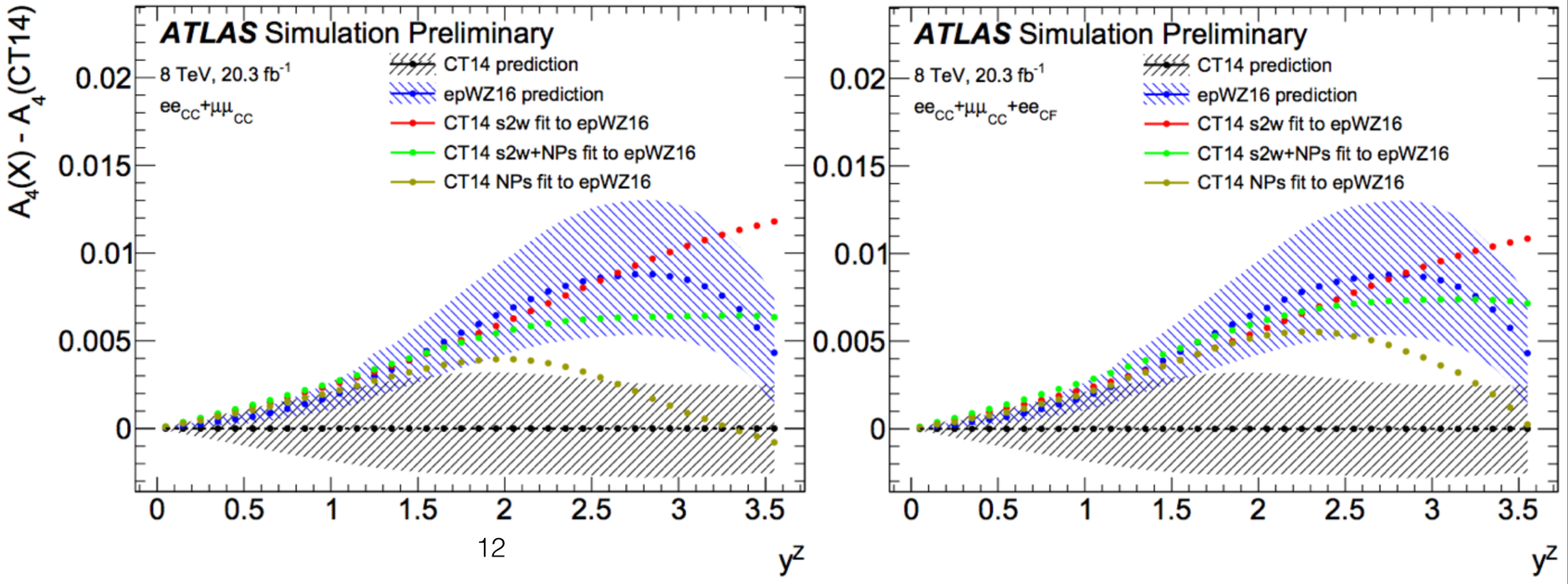

Table of $\sin^2\theta_W$-level non-closure

- Compare closure of $\sin^2\theta_W$ for CC-only and CC+CF, before and after PDFs are free in the fit
- For CC-only, can compare to PDF uncertainty in recent CMS $\sin^2\theta_W$ measurement, ~30×10^{-5}
- Differences mostly within 1σ of PDF uncertainty, with exception of epWZ16 and others, which can be 2-3σ away
- Closures on left are mostly symmetric, but asymmetries can come in to numbers on right since PDF NPs are different between columns
- In some cases, closure becomes worse after PDFs are allowed to vary
- In some cases, there are large (several σ) differences between closure with and without PDF NPs

Closure in $\sin^2\theta_W$, $\times10^{-5}$

CC-only

Generated pseudodata	PDFs used for interpretation of A4 versus $\sin^2\theta_W$									
	Before PDF constraint					After PDF constraint				
	CT10	CT14	MMHT14	NNPDF31	epWZ16	CT10	CT14	MMHT14	NNPDF31	epWZ16
CT10	-	33	-8.	-7	130	-	-18	22	17	-52
CT14	-33	-	-42	-41	98	27	-	44	39	-36
MMHT14	9	41	-	2	137	-29	-35	-	-4	-70
NNPDF31	8	40	-1	-	136	-16	-28	8	-	-53
epWZ16	-139	-103	-148	-148	-	87	44	93	86	-

CC+CF

Generated pseudodata	PDFs used for interpretation of A4 versus $\sin^2\theta_W$									
	Before PDF constraint					After PDF constraint				
	CT10	CT14	MMHT14	NNPDF31	epWZ16	CT10	CT14	MMHT14	NNPDF31	epWZ16
CT10	-	20	2	11	109	-	3	19	19	52
CT14	-20	-	-18	-9	91	8	-	21	21	56
MMHT14	-1	18	-	9	108	-25	-11	-	1	31
NNPDF31	-10	9	-9	-	99	-14	-9	4	-	43
epWZ16	-116	-95	-114	-105	-	-44	-66	-42	-42	-

Summary ($\sin^2\theta_W$ part)

- Closure tests done between different PDF sets on pseudo-measurements of $\sin^2\theta_W$ with 8 TeV ATLAS data
- Asking the question: “If we use PDF set X to measure $\sin^2\theta_W$, but nature looks like PDF set Y, what bias in $\sin^2\theta_W$ would we get?”
- Answer: Mostly within 1σ, with the exception of epWZ16
  - Possibly due to not-flexible-enough parametrization used within the set
  - Differences wrt other sets driven in a large way by W-asymmetry measurements at Tevatron
- Fits can absorb much of the difference between PDF sets, largely driven by fitting A_4 vs m^Z, to a smaller extent A_4 vs y^Z
- ee_{CF} channel can mitigate much of the non-closure in $\sin^2\theta_W$ due to high y^Z region balancing out differences between PDF sets
- These studies show that reaching non-closure values below $10\text{x}10^{-5}$ which would be needed for the long-term measurements of $\sin^2\theta_W$ at the LHC will require additional constraints from data on PDF sets
  - Possibly the most sensitive region related to the measurement $\sin^2\theta_W$ is that at high y^Z, typically where the acceptance of LHCb is the largest, but where also ATLAS and CMS should be able to contribute, albeit with larger experimental systematics than in the lower y^Z range

Fixed-order predictions and PDF fits

- Most precise cross sections and ratios measured by ATLAS :
  - W+, W- and Z cross sections at 7 TeV: experimental precision ~0.5% (excl. Lumi)
  - Ratios are even better thanks to cancellation of Luminosity uncertainty, partial cancellation of experimental systematic uncertainties
  - Ratios also provide the most sensitive tests of PDFs

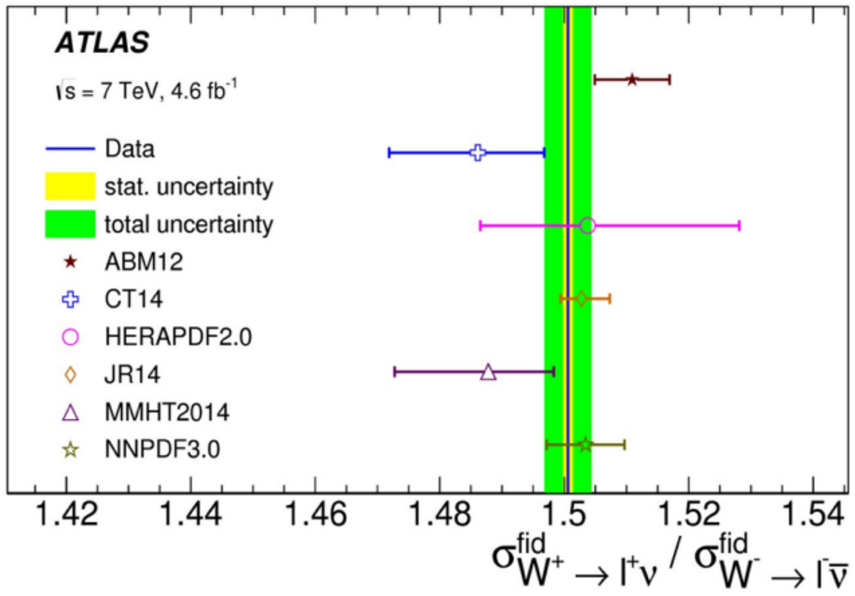

~0.3%

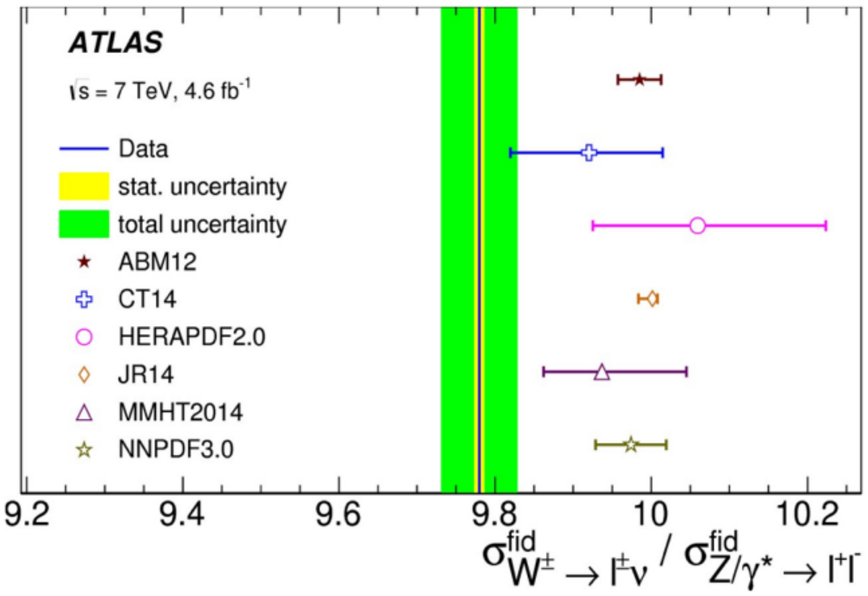

~0.5%

Fixed-order predictions and PDF fits

- QCD fits are generally performed comparing the data to PDFs convolved with partonic cross sections predicted at fixed order. These are characterized by an unrealistic boson pT distribution, diverging towards lower pT.

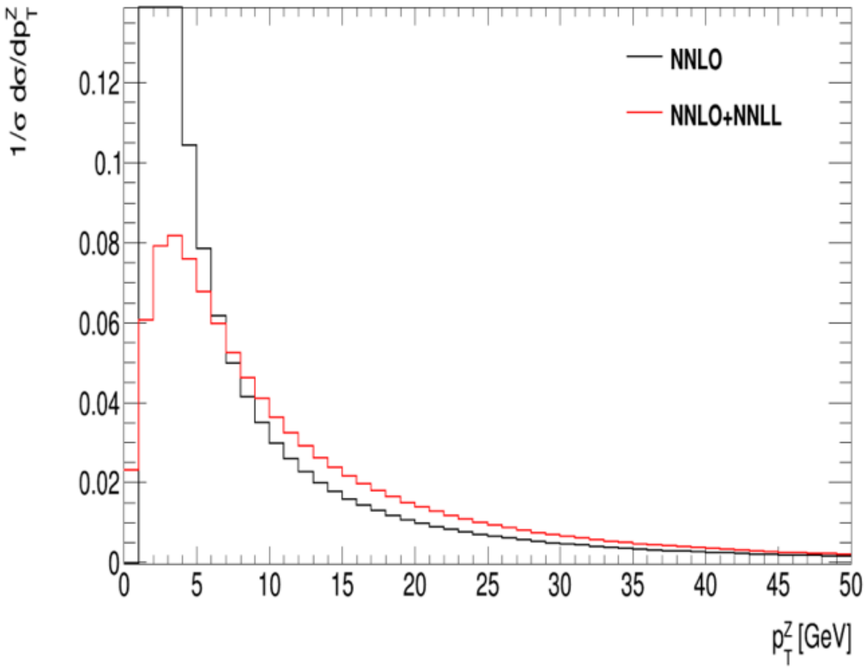

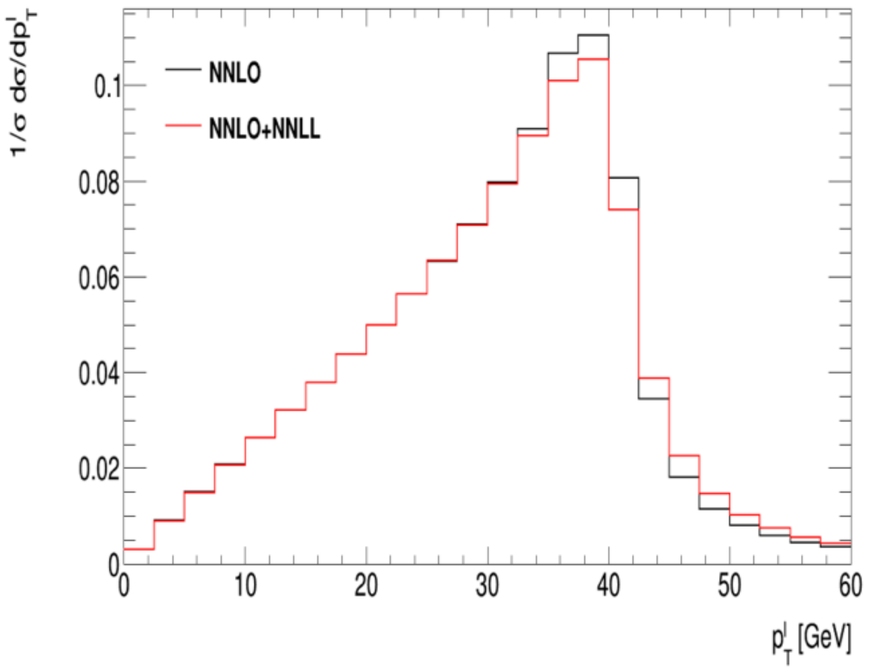

- Fiducial cross section calculations integrate over this distribution. Is there an impact on the accepance (esp. of p_T^l cuts)?

Fixed-order predictions and PDF fits

- Compared fiducial cross sections at various orders (NLO vs. NLO+NLL; NNLO vs. NNLO+NNLL), imposing that the total cross sections be identical in fixed-order and resummed calculations.
- Ratio between resummed and foxed-order fiducial cross sections; for W :

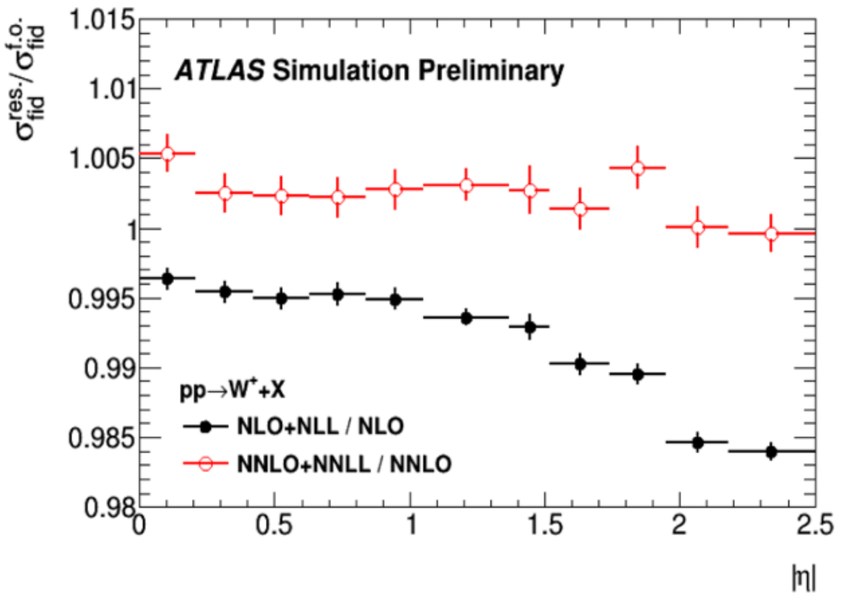

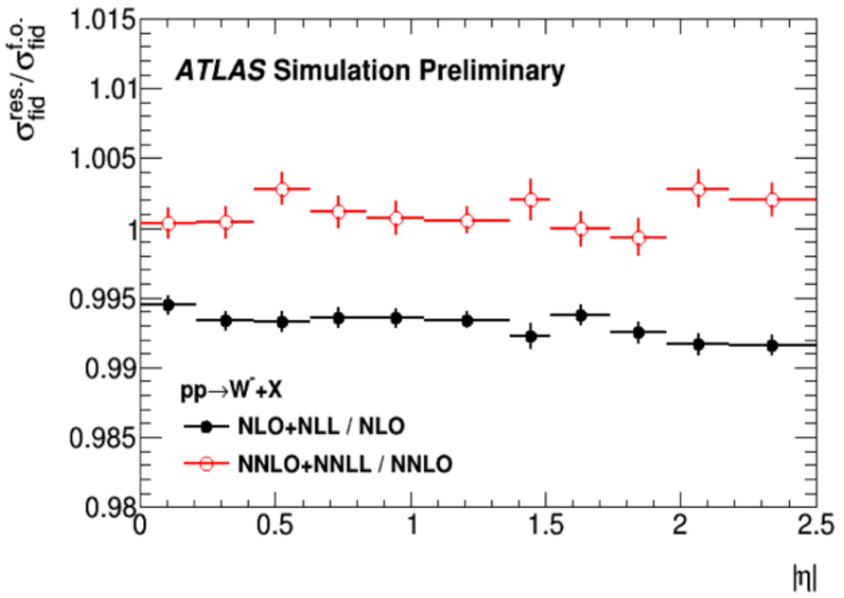

- Effects are O(1—1.5%) at NLO, and still O(0.5%) at NNLO

Fixed-order predictions and PDF fits

- Compared fiducial cross sections at various orders (NLO vs. NLO+NLL; NNLO vs. NNLO+NNLL), imposing that the total cross sections be identical in fixed-order and resummed calculations.
- Ratio between resummed and foxed-order fiducial cross sections; for Z :

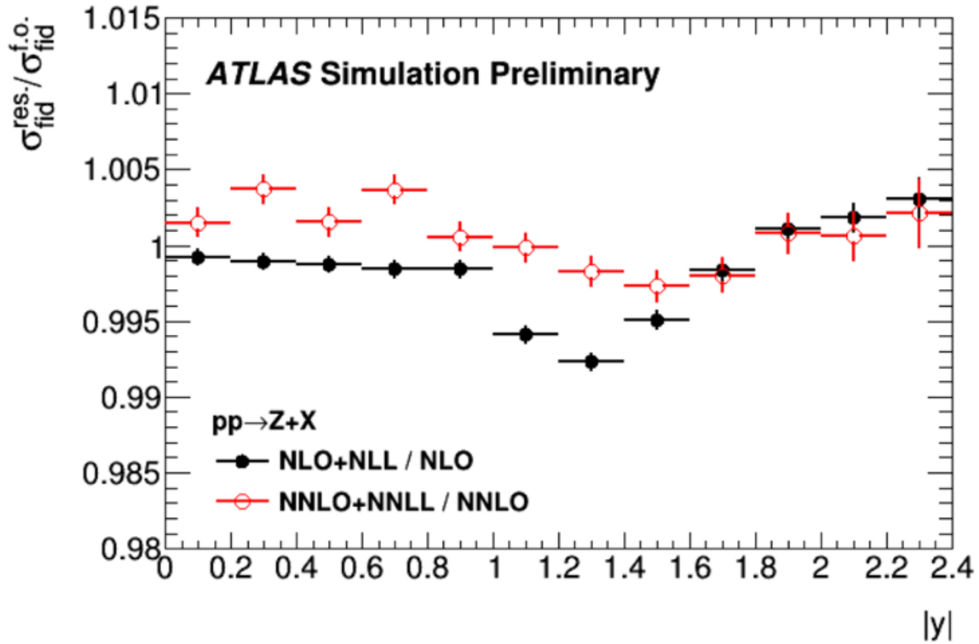

  - Effects are O(1—1.5%) at NLO, and still O(0.5%) at NNLO

Summary on resummation corrections

- For a few observables, the effect of missing resummation corrections matches the experimental precision of the measurements.

- We suggest to start incorporating these effects (and the corresponding uncertainties) when relevant for the interpretation of future high-precision measurements.

BACKUP

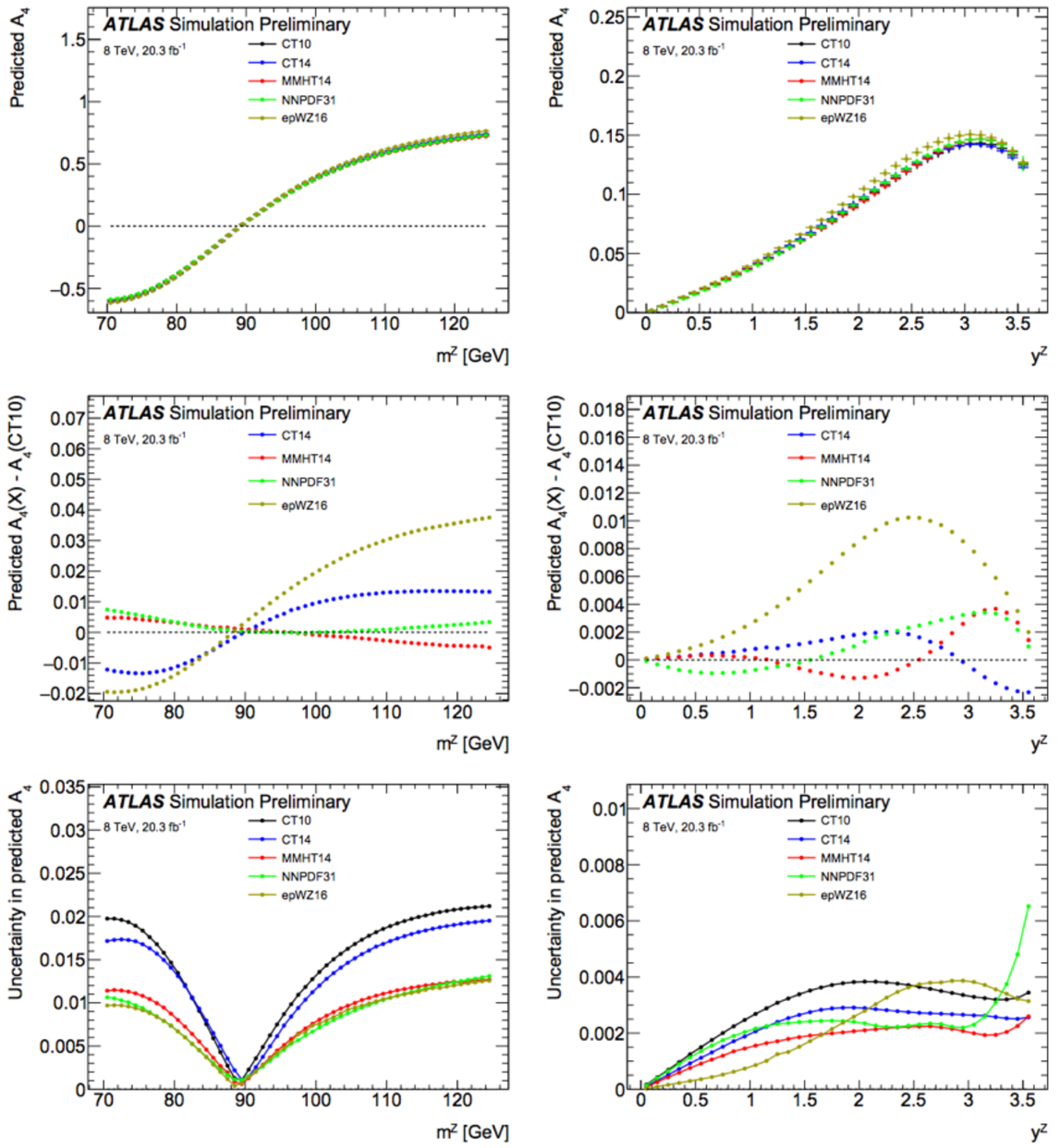

Figure 1: For different PDF sets, distributions of the predicted angular coefficient A_4 (top), of the difference between the various predictions and a reference one chosen as the CT10 PDF set (middle), and uncertainties in A_4 obtained from the different PDF sets (bottom). The distributions are shown as a function of the dilepton mass m^Z (left) and of the dilepton rapidity y^Z (right).

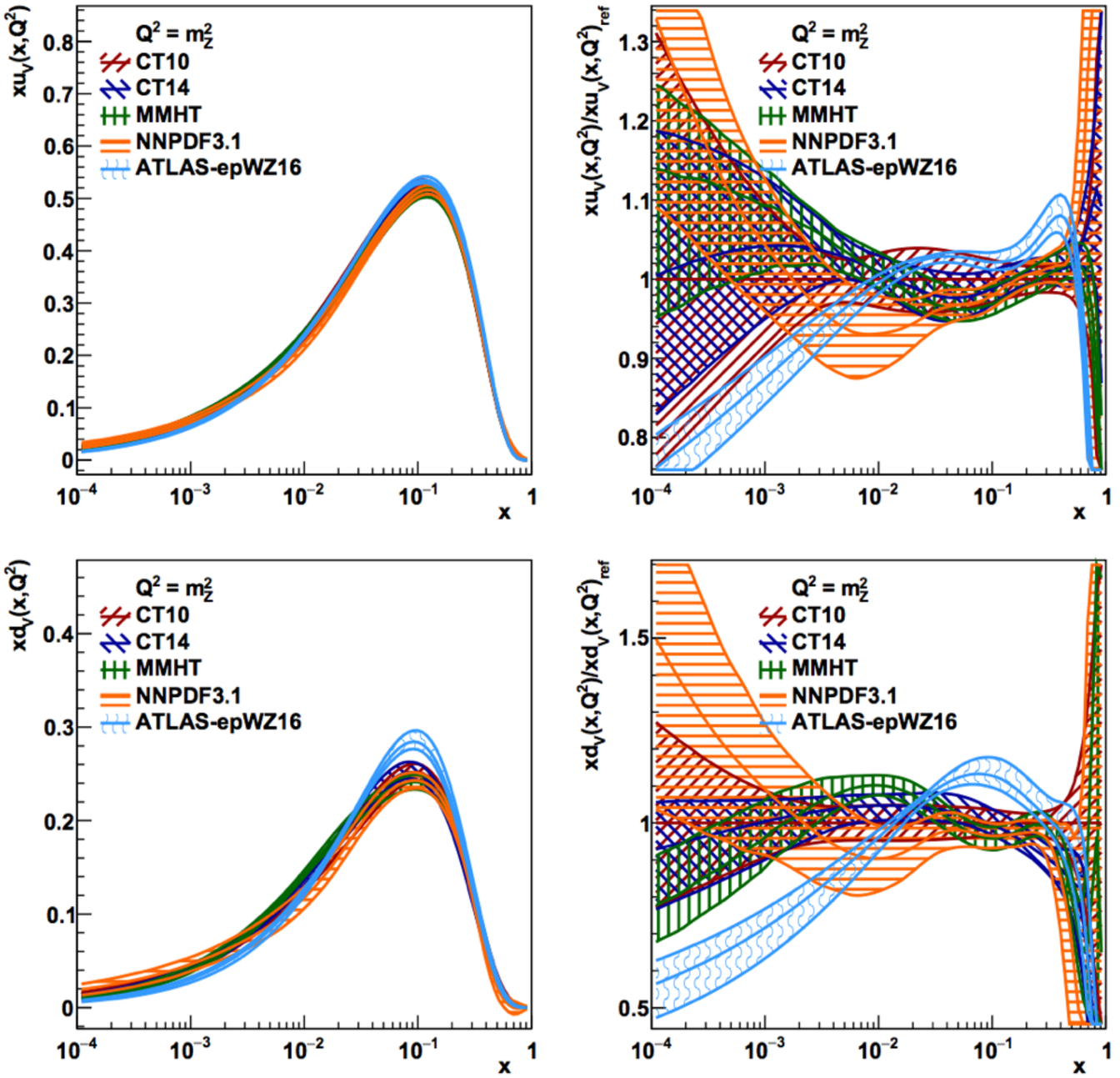

Figure 2: For the PDF sets considered in this note, distributions of the expected contributions from the up (top) and down (bottom) valence quarks of the proton as a function of x at the scale of the Z-boson, $Q^2 = m_Z^2$ (left). Also shown are the ratios of these distributions to the corresponding reference one of Ref. [6] (right).

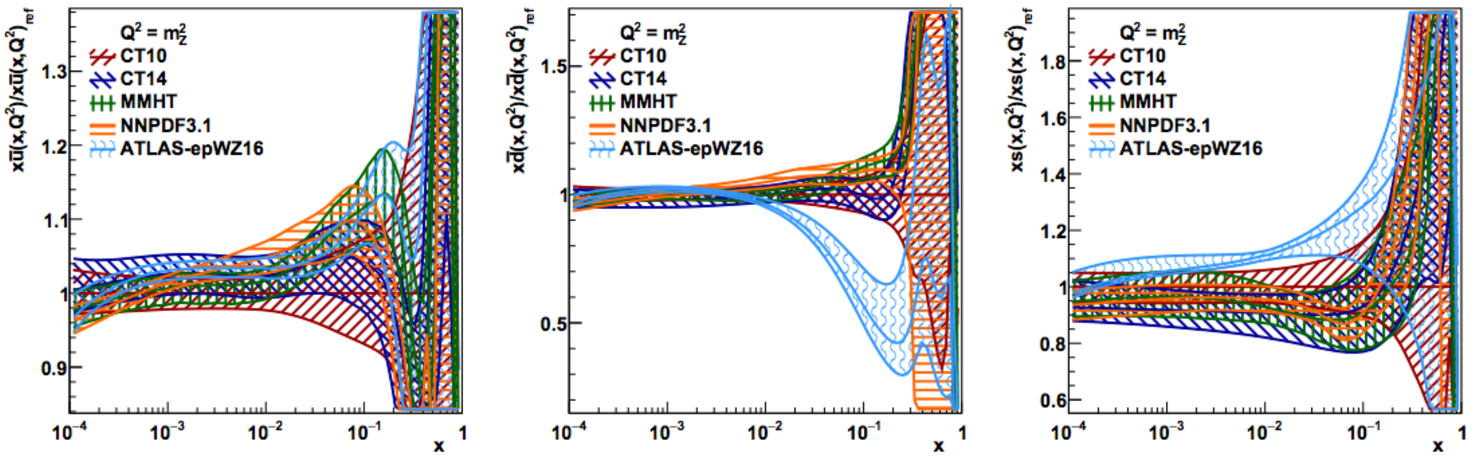

Figure 3: For the PDF sets considered in this note, ratios with respect to the corresponding reference distributions of Ref. [6] for the sea quarks: up (left), down (middle), and strange (right).

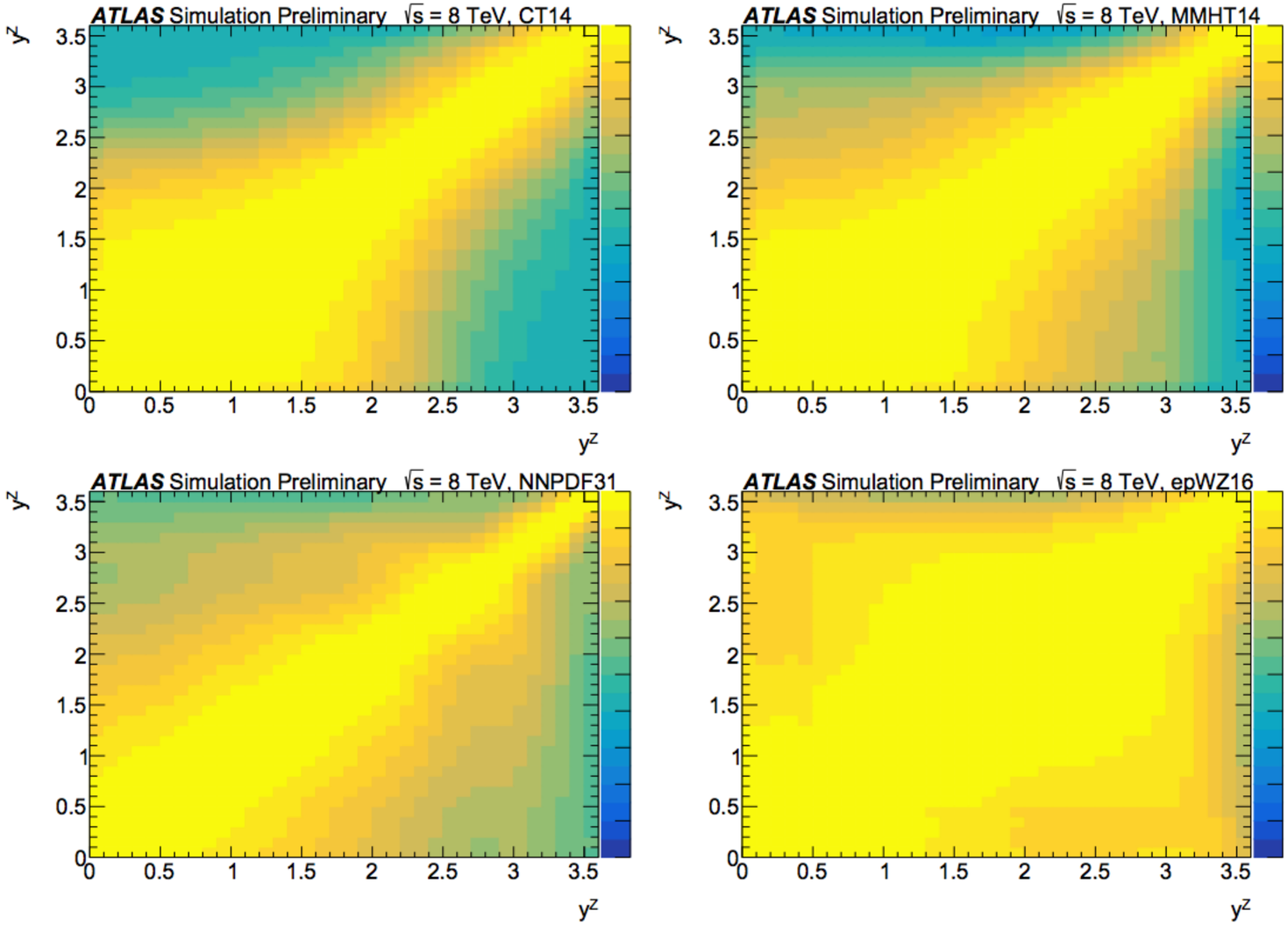

Figure 4: Correlations between the predicted angular coefficient A_4 as a function of y^Z, shown for the CT14 (top left), MMHT14 (top right), NNPDF31 (bottom left), and ATLAS epWZ16 (bottom right) PDF seta.

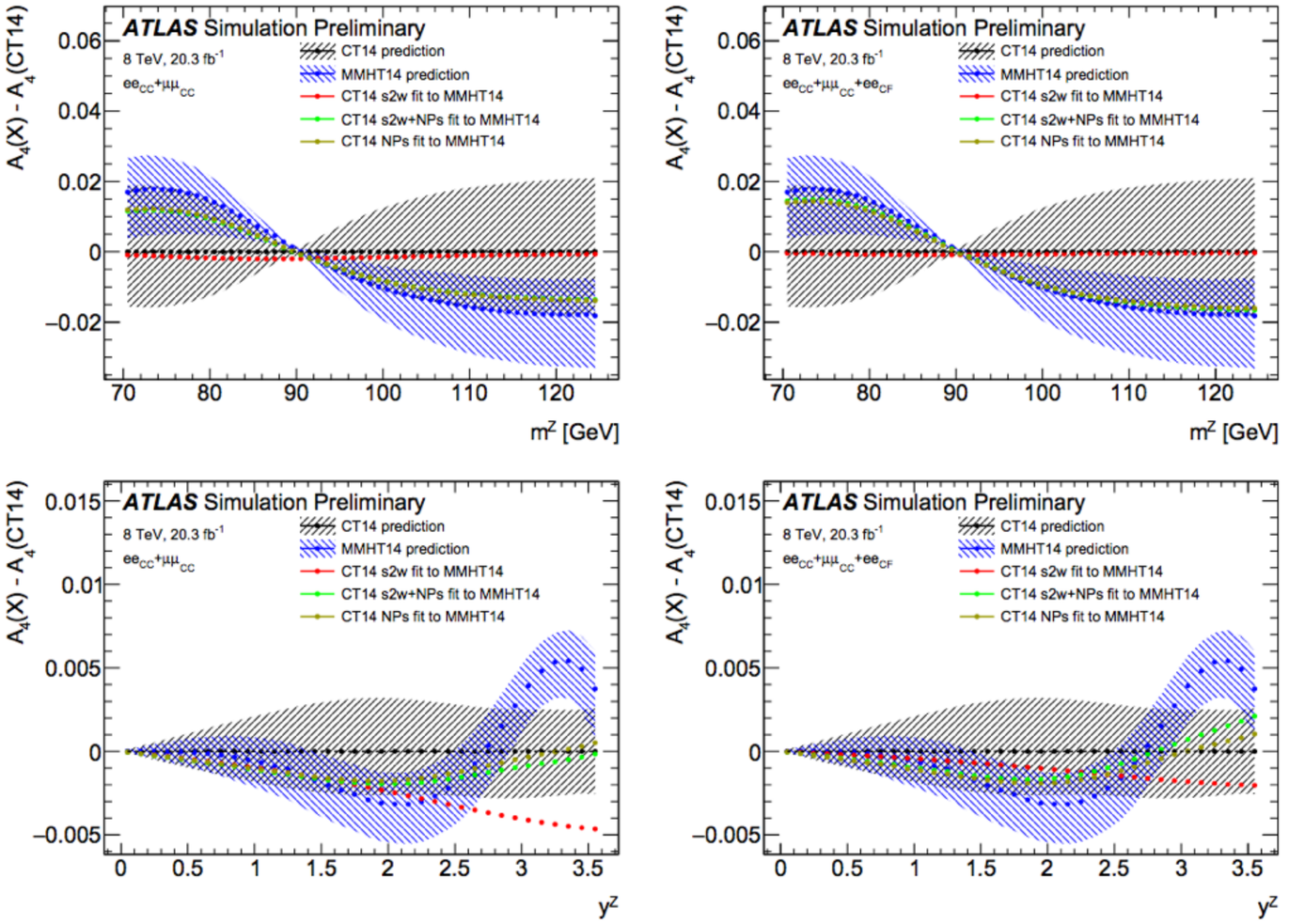

Figure 5: Differences between the fitted angular coefficient A_4 and the predicted value as a function of m^Z (top) and of y^Z (bottom), using only leptons in the central region (left) and including also electrons in the forward region (right). The reference prediction used for the fit is that of the CT14 PDF set (black points with shaded PDF uncertainty band) centred at zero) and the pseudodata (blue points with shaded PDF uncertainty band) are obtained using MMHT14. Three fit results are shown: the first one (red points labelled as "s2w fit"), where only the parameter of interest, $\sin^2\theta_W$, is allowed to vary, the second one (brown points labelled as "NPs fit"), where only the PDF parameters are allowed to vary, and finally the complete fit (green points labelled as "s2w+NPs fit") where all parameters are allowed to vary together. As explained in the text, only statistical uncertainties, as expected from the ATLAS 8 TeV dataset, are included in the fits (systematic experimental and theoretical uncertainties from the actual expected measurement of A_4 are not included here to maximise the sensitivity to the choice of PDFs and their related uncertainties).

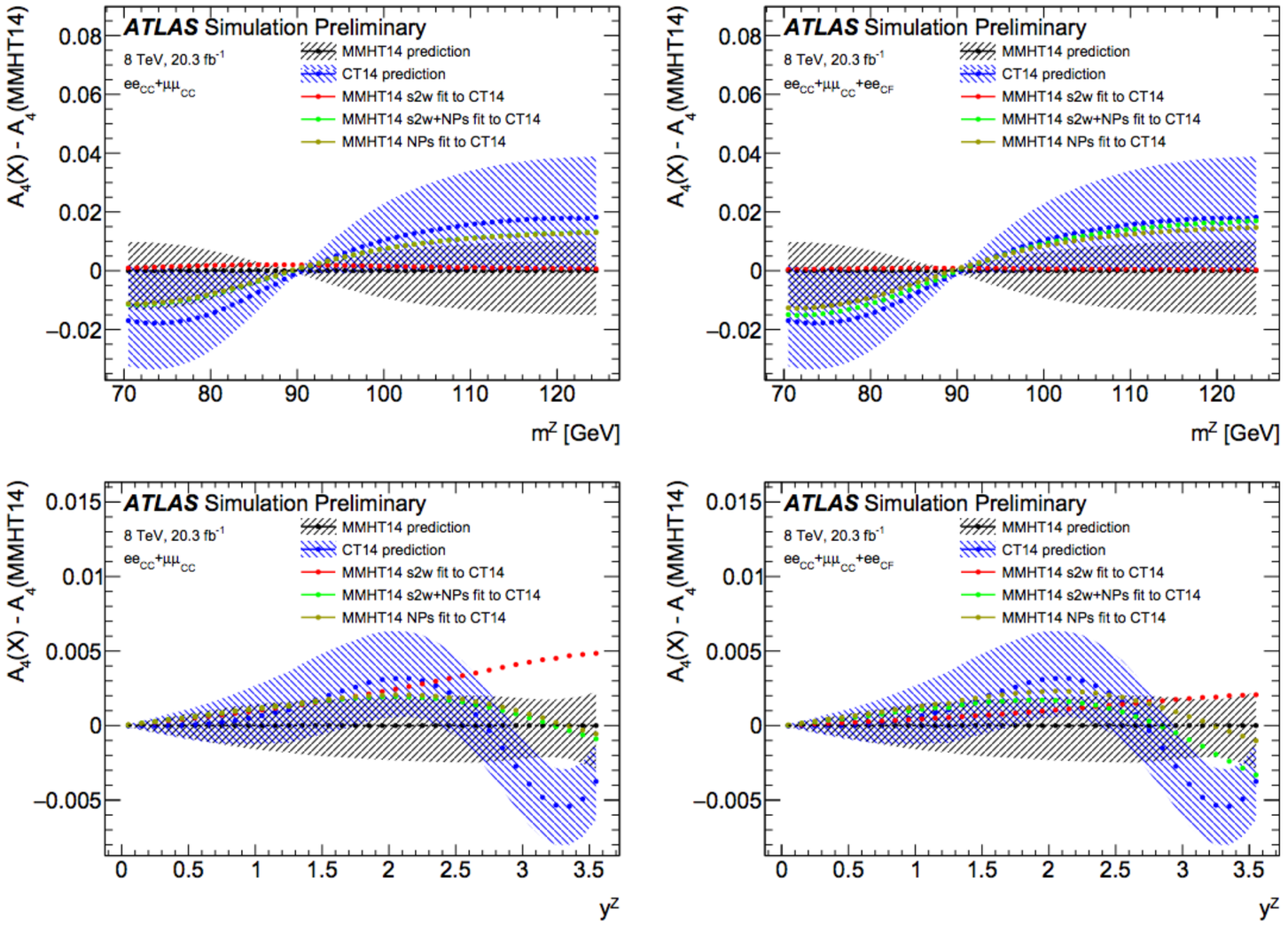

Figure 6: Same as Fig. 5, but with the PDF sets reversed, i.e. using the MMHT14 PDF set as the reference prediction to which the pseudodata obtained using the CT14 PDF set are fitted.

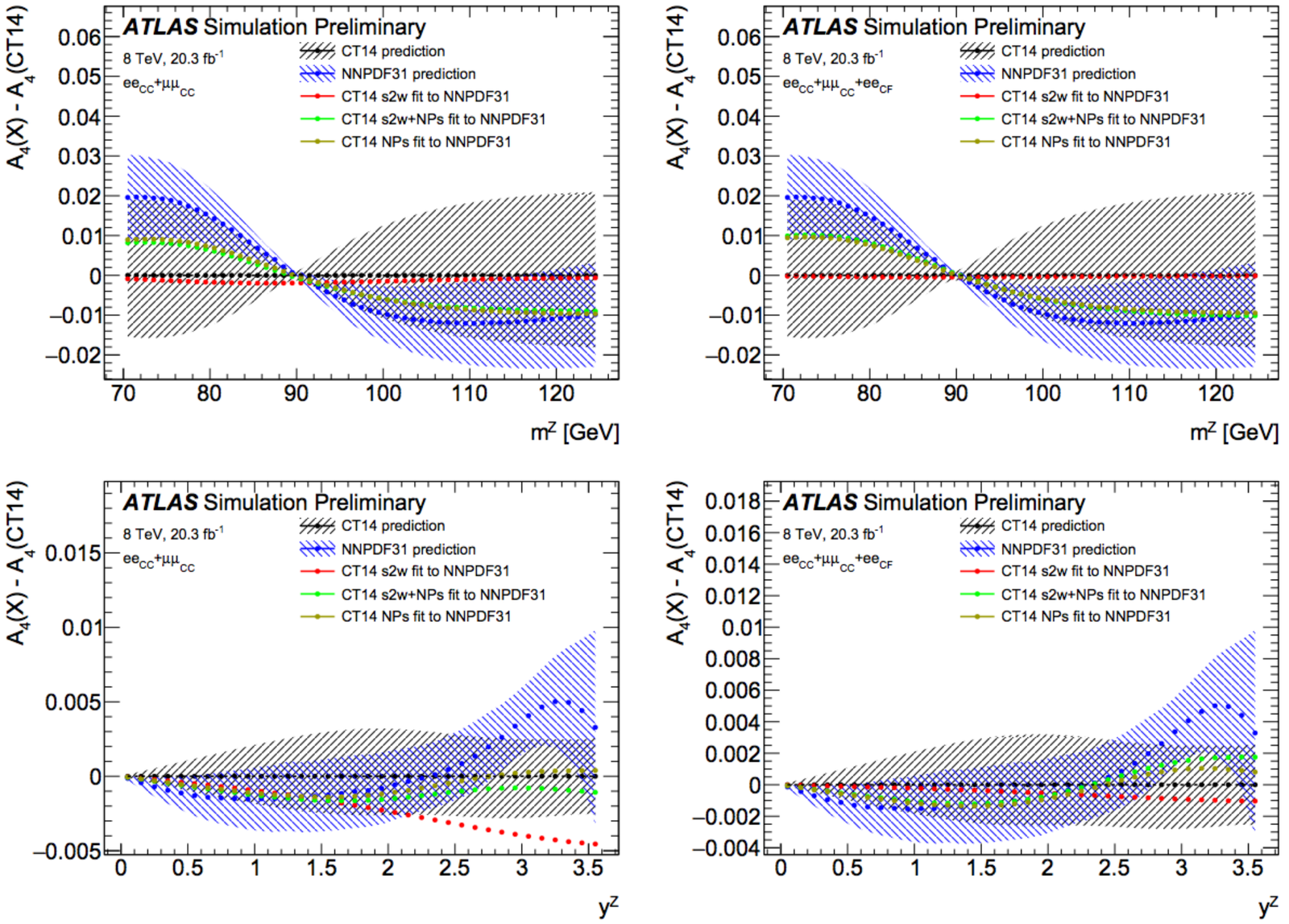

Figure 7: Same as Fig. 5, but with the MMHT14 PDF set replaced by the NNPDF31 PDF set.

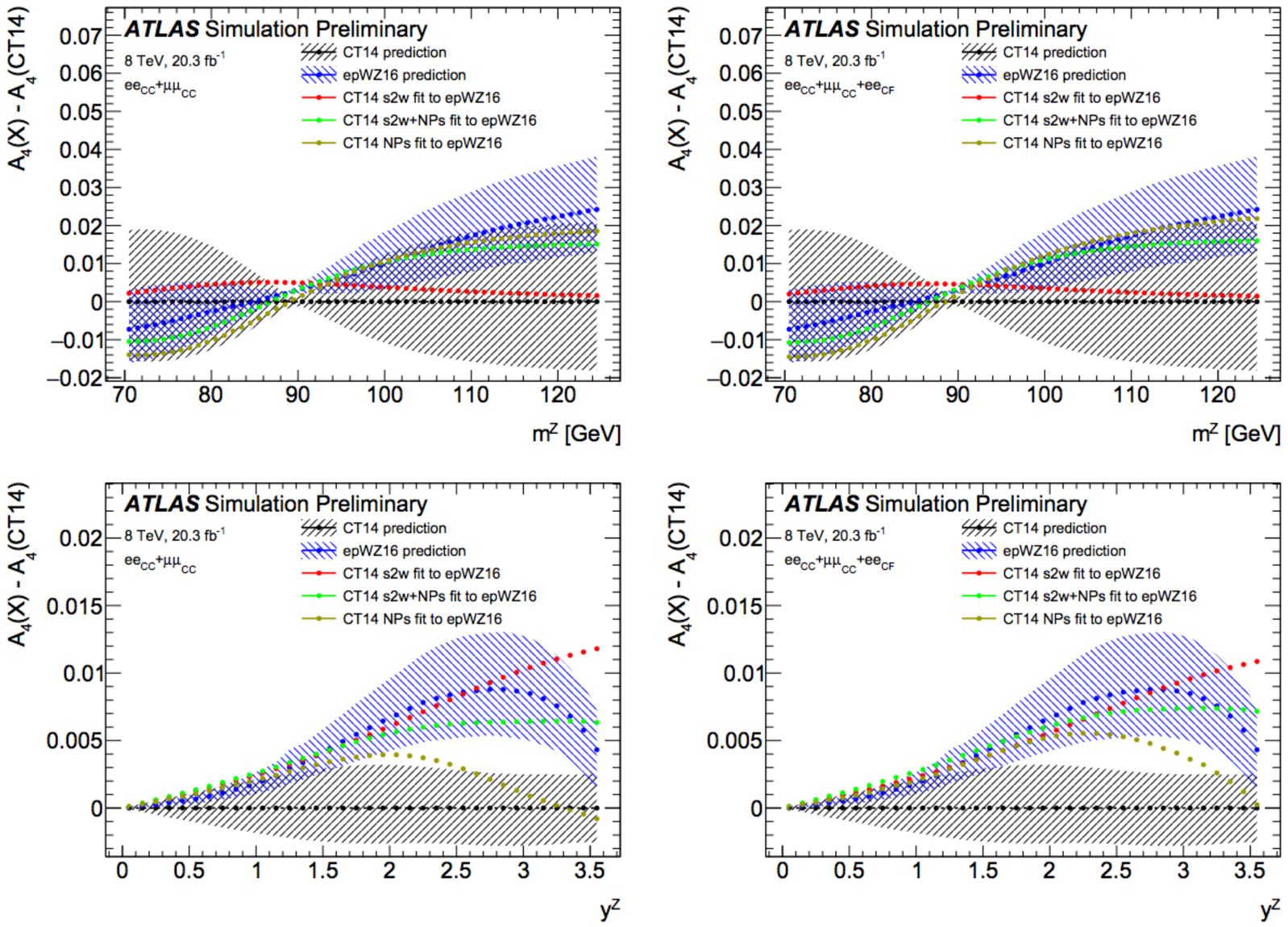

Figure 8: Same as Fig. 5, but with the MMHT14 PDF set replaced by the ATLAS epWZ16 PDF set.

Table 1: Coefficients a and b used for different PDF sets to predict the angular coefficient A_4 as a function of $\sin^2\theta_W$ using a linear function $A4 = a \times sin^2\theta_W + b$, for A_4 integrated over all the measurement bins as defined in the text.

PDF set	CT10	CT14	MMHT14	NNPDF31	ATLAS epWZ16
a	-4.5499	-4.6531	-4.5809	-4.5551	-4.8477
b	1.1234	1.1485	1.1313	1.1251	1.1974

Table 2: Differences between the predicted and fitted values of the angular coefficient A_4, expressed in units of 10^{-3} for A_4 integrated over all the measurement bins as defined in the text. The expected statistical precision of this measurement is $\sim 10^{-3}$. The fit results are shown for all dilepton pairs including the events with one electron in the forward region and for all possible pairs of PDF sets considered, where one set is used to generate pseudodata and the second one is used to perform the fit. For each pair of PDF sets, the reference prediction for A_4 is given together with its expected uncertainty arising only from the PDF uncertainties. The table then shows the differences in A_4 between the pseudodata and the reference, together with differences obtained from the fit results for the three cases also illustrated in e.g. Fig. 5: the case labelled as "Fit with s2w" where the only parameter varied in the fit is the value of $\sin^2\theta_W$, the case labelled as "Fit with NPs", where only the PDF parameters are varied in the fit, and finally the case of the complete fit labelled as "Fit with s2w+NPs", where the PDF parameters and $\sin^2\theta_W$ are varied together. As explained in the text, only statistical uncertainties, as expected from the ATLAS 8 TeV dataset, are included in the fits (systematic experimental and theoretical uncertainties from the actual expected measurement of A_4 are not included here to maximise the sensitivity to the choice of PDFs and their related uncertainties).

Pseudodata PDF set: CT10				
Interp. model PDF set	CT14	MMHT14	NNPDF31	epWZ16
Interp. model pred.	71.2	70.6	70.4	74.9
PDF syst. on interp. pred.	+1.9 / -1.7	+1.4 / -1.8	+1.7 / -1.7	+1.8 / -1.5
Difference with respect to interp. model prediction				
Pseudo-data pred.	-1.1	-0.6	-0.4	-4.9
Fit with s2w	-0.9	-0.1	-0.5	-5.3
Fit with NPs	-0.8	0.5	-0.1	-3.7
Fit with s2w+NPs	-0.8	0	-0.5	-5.1
Pseudodata PDF set: CT14				
Interp. model PDF set	CT10	MMHT14	NNPDF31	epWZ16
Interp. model prediction	70.0	70.6	70.4	74.9
PDF syst. on interp. pred.	+2.8 / -2.5	+1.4 / -1.8	+1.7 / -1.7	+1.8 / -1.5
Difference with respect to interp. model prediction				
Pseudo-data pred.	1.1	0.5	0.7	-3.8
Fit with s2w	0.9	0.8	0.4	-4.4
Fit with NPs	1.0	1.5	0.8	-2.8
Fit with s2w+NPs	0.8	0.9	0.3	-4.3
Pseudodata PDF set: MMHT14				
Interp. model PDF set	CT10	CT14	NNPDF31	epWZ16
Interp. model pred.	70.0	71.2	70.4	74.9
PDF syst. on interp. pred.	+2.8 / -2.5	+1.9 / -1.7	+1.7 / -1.7	+1.8 / -1.5
Difference with respect to interp. model prediction				
Pseudo-data pred.	0.6	-0.5	0.2	-4.3
Fit with s2w	0.1	-0.8	-0.4	-5.2
Fit with NPs	-0.4	-1.0	-0.4	-4.2
Fit with s2w+NPs	0.1	-0.7	-0.4	-5.0
Pseudodata PDF set: NNPDF31				
Interp. model PDF set	CT10	CT14	MMHT14	epWZ16
Interp. model pred.	70.0	71.2	70.6	74.9
PDF syst. on interp. pred.	+2.8 / -2.5	+1.9 / -1.7	+1.4 / -1.8	+1.8 / -1.5
Difference with respect to interp. model prediction				
Pseudo-data pred.	0.4	-0.7	-0.2	-4.5
Fit with s2w	0.5	-0.4	0.4	-4.8
Fit with NPs	0.1	-0.5	0.5	-3.4
Fit with s2w+NPs	0.4	-0.3	0.5	-4.6
Pseudodata PDF set: epWZ16				
Interp. model PDF set	CT10	CT14	MMHT14	NNPDF31
Interp. model pred.	70.0	71.2	70.6	70.4
PDF syst. on interp. pred.	+2.8 / -2.5	+1.9 / -1.7	+1.4 / -1.8	+1.7 / -1.7
Difference with respect to interp. model prediction				
Pseudo-data pred.	4.9	3.8	4.3	4.5
Fit with s2w	5.3	4.4	5.2	4.8
Fit with NPs	4.3	3.0	4.4	3.8
Fit with s2w+NPs	5.2	4.3	5.5	4.7

Table 3: Summary of fit results of pseudodata created with various PDFs for the distribution of the angular coefficient A_4 as reconstructed from $Z \to ll$ decays in the central region of the detector, i.e. for electrons and muons with $|\eta| < 2.5$. The predictions used for the fit are performed with different PDFs. The uncertainties are purely statistical to maximise possible non-closure effects as explained in the text, and their magnitude is as expected from the 8 TeV Z-boson dataset .The results are shown in terms of bias on the weak mixing angle in units of 10^{-5}.

Generated pseudodata	PDFs used for interpretation of A4 versus $\sin^2\theta_W$									
	Before PDF constraint					After PDF constraint				
	CT10	CT14	MMHT14	NNPDF31	epWZ16	CT10	CT14	MMHT14	NNPDF31	epWZ16
CT10	-	33	-8.	-7	130	-	-18	22	17	-52
CT14	-33	-	-42	-41	98	27	-	44	39	-36
MMHT14	9	41	-	2	137	-29	-35	-	-4	-70
NNPDF31	8	40	-1	-	136	-16	-28	8	-	-53
epWZ16	-139	-103	-148	-148	-	87	44	93	86	-

Table 4: Same as Table 3, but including in addition $Z \to ee$ decays with one electron in the forward region of the detector, i.e. with $2.5 < |\eta| < 4.9$.

Generated pseudodata	PDFs used for interpretation of A4 versus $\sin^2\theta_W$									
	Before PDF constraint					After PDF constraint				
	CT10	CT14	MMHT14	NNPDF31	epWZ16	CT10	CT14	MMHT14	NNPDF31	epWZ16
CT10	-	20	2	11	109	-	3	19	19	52
CT14	-20	-	-18	-9	91	8	-	21	21	56
MMHT14	-1	18	-	9	108	-25	-11	-	1	31
NNPDF31	-10	9	-9	-	99	-14	-9	4	-	43
epWZ16	-116	-95	-114	-105	-	-44	-66	-42	-42	-

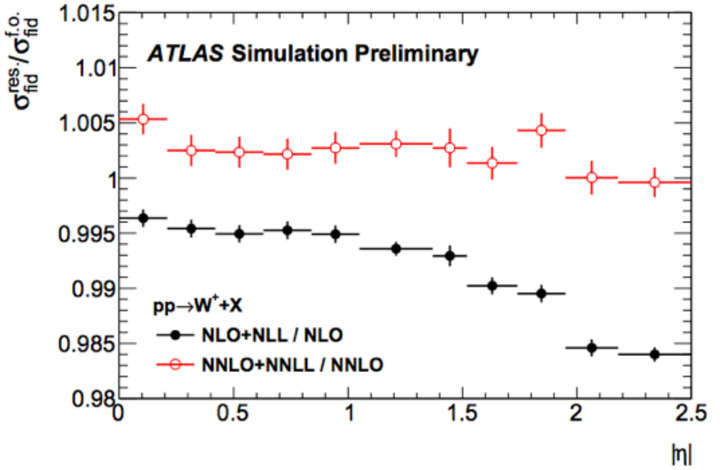

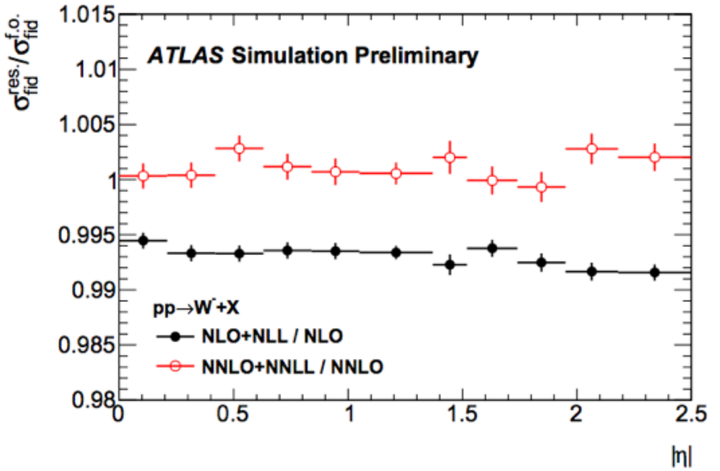

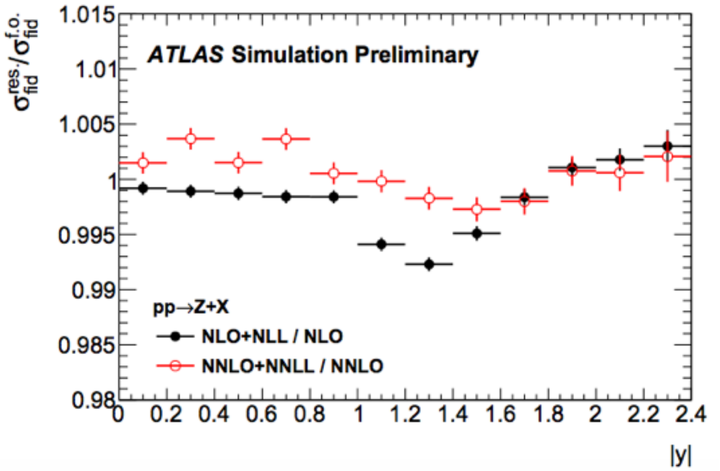

Figure 9: Ratio between resummed and fixed-order fiducial cross sections, for W^+ (top), W^- (middle) and Z (bottom) boson production. These cross sections are shown differentially as a function of lepton pseudorapidity $|\eta|$ for W-boson decays and of dilepton rapidity y for Z-boson decays. The full (black) and open (red) circles show the NLO+NLL to NLO and NNLO+NNLL to NNLO ratios from theoretical calculations, respectively, as explained in the text. These fiducial cross sections are defined by $p_{\mathrm{T}}^{\ell} > 25$ GeV, $|\eta_{\ell}| < 2.5$, $p_{\mathrm{T}}^{\nu} > 25$ GeV and $m_{\mathrm{T}} > 40$ GeV for $W \to \ell\nu$ decays, and by $p_{\mathrm{T}}^{\ell} > 20$ GeV, $|\eta_{\ell}| < 2.5$ and $66 < m_{\ell\ell} < 116$ GeV for $Z \to \ell\ell$ decays.